

**Final Report for NSF Award ATM- 0129892**

**Optimal Utilization and Impact of Water Vapor and Other High  
Resolution Observations in Storm-Scale QPF**

Prof. Ming Xue<sup>1,2</sup>, Principal Investigator  
Prof. Frederick H. Carr<sup>1,2</sup>, Co-Principal Investigator  
Prof. Alan Shapiro<sup>1,2</sup>, Co-Principal Investigator  
Dr. Keith Brewster<sup>1</sup>, Co-Principal Investigator  
Dr. Jidong Gao<sup>1</sup>, Co-Principal Investigator

<sup>1</sup>Center for Analysis and Prediction of Storms and <sup>2</sup>School of Meteorology  
University of Oklahoma

120 David Boren Blvd  
Norman OK 73072

**August 2006**

Contacting e-mail: [mxue@ou.edu](mailto:mxue@ou.edu)

## 1 Introduction

According to the original proposal, this project was to perform moisture sensitivity and data assimilation studies with focus on the storm scale and quantitative precipitation. The project had the following goals: 1) Develop and apply variational techniques for the analysis and assimilation of water and related diabatic fields; 2) Study the impact of high-resolution observations of water vapor and hydrometeor content on the forecasting of convective storm morphology and precipitation; 3) Develop and evaluate techniques for estimating error characteristics of numerical forecasts at the convective scale; 4) Apply single Doppler velocity and thermodynamic retrieval algorithms to mobile radar data collected during IHOP; 5) Provide real-time, high-resolution (2-3 km) analysis and forecasts to assist IHOP field operations. Significant accomplishments were achieved in the goal areas, including many publications produced. These are first summarized in section 2 in terms of published papers. More specific results are presented in section 3.

## 2 Publications and Other Research Accomplishments

This grant provided full or partial support for 7 graduate students (Paul Nutter, Geoffrey Stano, Mingjing Tong, Haixia Liu, Ying Xiao, Ming Hu and Daniel Dawson) and 2 post-doctoral scientists (Jinzhong Min and William Martin). Three Ph.D. degrees (Nutter, Tong and Hu) and 2 M.S. degrees (Stano and Dawson) were earned with the support of the grant. In addition, Ying Xiao completed his Ph.D. degree in computer science after a one-year appointment within this project working as a graduate student programmer. The project PIs, scientists and students published or have submitted more than 50 refereed papers and several dozen conference papers. The most relevant results are briefly summarized here.

The first group of papers focuses on radar wind retrieval, quality control, and analysis. These papers include Shapiro et al. (2002; 2003) and Gao et al. (2004c; 2006c) which reported advances in single Doppler velocity retrieval (SDVR), Gao et al (2002; 2003; 2004a) reported the development of three-dimensional variational (3DVAR) assimilation of radar data for small-scale nonhydrostatic flows, Gao et al. (2004) developed a new variational method for retrieving vertical wind profiles from the azimuthal gradient of radial velocity data, and Bi et al. (2002) on the quality control of radar VAD winds and Level-II radar data in the presence of migratory birds. Gao and Drogemeier (2004) described and tested a new variational velocity dealiasing algorithm, and, more recently, Gao et al. (2006a; 2006b) examined various radar ray path equations and approximations for use in radar data assimilation (DA). More recent improvements to the ARPS modeling and DA systems together with earlier results of applying ADAS (ARPS Data Analysis System, Brewster 2002) and cloud analysis to the March 2000 Fort Worth tornadic thunderstorm case are reported in Xue et al. (2003). Hu and Xue (2002) also studied the sensitivity of predicted tornadic storms in this case to changes in environmental conditions.

Co-PI Keith Brewster completed the development, testing and formal publication of a procedure for correcting phase errors in the analysis background for storm-scale DA and NWP (Brewster 2003a; 2003b). He also improved the complex cloud analysis scheme and developed a new diabatic perturbation scheme for ADAS. The newly developed ARPS 3DVAR system (Gao et al. 2004a) and the improved cloud analysis scheme led to improvements in forecasts of the

March 2000 Fort Worth tornadic supercell storm case (Hu et al. 2004; Hu et al. 2006a; Hu et al. 2006b). These papers also analyzed in detail the role of a divergence constraint in the 3DVAR system and the effects of various improvements in the cloud analysis. The assimilation of reflectivity data through cloud analysis in a cycled mode was shown to be of first order importance, and the proper specification of thermal perturbations in the procedure was key. Ming Hu is a Ph.D. student initially supported by our prior NSF grant ATM9909007 and, more recently, by the FAA and this grant.

The data impact study by Dan Dawson (a recipient of NSF and National Defense Graduate Research Fellowships who finished his M.S. in 2004 and is continuing for his Ph.D. under the PI) further demonstrated the positive impact of cloud analysis using reflectivity data from multiple radars and the assimilation of other special sources of data (e.g., surface observations from over 10 regional mesonets) collected during the 2002 IHOP field campaign for the forecast of a mesoscale convective system (MCS) (Dawson and Xue 2004, 2006). A significant positive impact, of cloud analysis in particular, was found to last for at least 12 hours in this case. The positive impact of a simplified cloud analysis was also demonstrated by month-long precipitation verifications in Souto et al. (2003). In addition, Souto et al. (2003) and Sheng et al. (2006) also examined the impact of assimilating radar data on the prediction of various precipitation systems,

Ph.D. student Paul Nutter, supported by this grant in the final year of his Ph.D. program and co-advised by the PI and Dave Stensrud of the National Severe Storms Laboratory (NSSL), obtained his Ph.D. in 2003 and recently started a teaching appointment at the University of North Colorado. He systematically analyzed the effects of lateral boundary condition perturbations on the dispersion of regional ensemble forecasts (Nutter et al. 2002; Nutter 2003; Nutter et al. 2004a; Nutter et al. 2004b). Further, he proposed and tested a method for systematically introducing boundary condition perturbations that restore much of the ensemble dispersion (Nutter et al. 2004c). The work also developed a new and very useful equation that links error variance spectra to ensemble spread while accounting for spatial and ensemble mean errors.

Ph.D. student, Haixia Liu developed a new univariate 3DVAR system for analyzing water vapor from GPS slant-path water vapor observations (Liu and Xue 2004, 2006a). Unique aspects of this work include the use of flow-dependent background error structures that are modeled by anisotropic explicit or recursive spatial filters. Observation system simulation experiments (OSSEs) performed for an IHOP dryline case (19 June 2002) clearly demonstrated the significant positive impact from the use of the flow-dependent background error. The analysis system was also shown, among other things, to be robust, even in the presence of observational errors and/or with a poor analysis background. The recursive filter version of the anisotropic background error has also been implemented in our 3DVAR system, improving its computational efficiency. Analyses with the recursive filter show slightly better quality than those with an explicit filter. We believe this result is due to the improved positive definiteness property of the recursive filter. The results are summarized in an accepted manuscript (Liu et al. 2006a).

Ph.D. student, Mingjing Tong, developed an ensemble Kalman filter (EnKF) DA system based on the ARPS model for the assimilation of Doppler radar data as well as other sources of data (Tong and Xue 2005b). Tong and Xue (2004; 2005b), for the first time, assimilated both radial velocity and reflectivity data in a numerical model that contains multi-class ice microphysics. Their OSSEs demonstrated the superior ability of EnKF in accurately retrieving multiple microphysical species as well as wind and thermodynamic variables. Better results were obtained when both radial velocity and reflectivity data were assimilated. It was also shown that dynamically consistent background error covariances develop in the system even in the case

when the system is handicapped by being fed only reflectivity in the precipitation regions. A subsequent study (Xue et al. 2005b) further examined error growth in the EnKF system and showed that the covariance information derived from the ensemble plays a critical role in successful assimilation and retrieval.

In Xue et al. (2005b; 2006a), an improved version of our EnKF code was used to study the effectiveness and impact of assimilating data from a network of four low-cost radars planned for the Oklahoma test-bed of the recently established NSF Engineering Research Center (ERC) called CASA (Collaborative Adaptive Sensing of the Atmosphere, <http://casa.umass.edu>). The utility of these radars in providing coverage of the atmosphere below the coverage of the existing WSR-88D network was clearly demonstrated. The importance of storm propagation speed and radar scan frequency was also examined. Many additional issues such as beam geometry, adaptive scanning, and attenuation correction, are being studied using this tool, in support of CASA's mission. In addition, our EnKF system has been successfully used to perform microphysical parameter retrievals (Tong and Xue 2005a; Tong and Xue 2006b, a), and to assimilate real radar data for a tornadic supercell storm case (Xue et al. 2005a).

In support of the IHOP\_2002 field experiment, CAPS performed real time forecasts at 27, 9 and 3 km resolutions during the field experiment period (Xue et al. 2002). Detailed precipitation verifications were performed and presented at the Spring IHOP Science Meeting 2003 (Xue and Min 2003). The results clearly show improved precipitation forecast skill as the grid resolution increases. Graphical output of the ARPS forecasts remain on the web (<http://ihop.caps.ou.edu>) and all digital input and output data are kept online for easy access by subsequent studies.

To perform the proposed adjoint sensitivity studies, an adjoint code for a very recent, full, version of ARPS was developed with the help of a commercial automatic adjoint code generator, TAF (Transformation of Algorithms in Fortran), considered the best adjoint code generator in existence (Xiao et al. 2004; Xiao et al. 2005). So far, the ARPS is the most complex code for which the TAF has successfully generated a complete adjoint code. Initial test results are given in Xiao et al. (2005).

Post-doctoral scientist William Martin completed an innovative and unique (manuscript reviewers' words) initial condition sensitivity study using a very large (a total of 12,000 member) ensemble approach (Martin and Xue 2004) for the 24 May 2002 IHOP case of dryline convective initiation. By systematically perturbing a single variable in a finite patch of the domain of the initial condition for each ensemble member, the method produced detailed sensitivity maps of short-range QPF to boundary-layer moisture, winds and the soil moisture content. The method identified cases of extreme sensitivity; for example, a  $1 \text{ g kg}^{-1}$  water vapor perturbation over a  $27 \times 27 \times 1 \text{ km}^3$  volume at certain locations was found to make the difference between no precipitation and an intense convective storm. Physical explanations were also offered in the paper, as one reviewer commented, "I appreciated the physical understanding of the various sensitivities, something that has often been lacking in many previous sensitivity studies". Being based on nonlinear model runs, the technique is not subject to the limitation of linearization assumptions. In Martin and Xue (2006c), new, more efficient, methods are proposed that extend the method of Martin and Xue (2004).

The convective initiation processes of the same 24 May 2002 case were studied in depth in two other IHOP special issue papers (Xue and Martin 2006b; 2006a), through high-resolution (1 km) numerical simulations using ARPS and ADAS. In a reviewer's words, they are 'interesting papers with exciting results'. By assimilating high-density surface networks (e.g., the Texas Mesonet) and other special observations from IHOP, three series of convective cells initiated at

specific locations of the dryline were accurately predicted to within 20 min and 25 km of the true cells. The model also correctly predicted the lack of initiation of convection at the dryline-cold front triple point to the north, on which a large array of instruments were focused on that day. The evolution of the simulated dryline and the convective initiation process were analyzed in great detail. For the first time, the exact process by which boundary-layer eddies and horizontal convective rolls interact with the dryline convergence line to determine the exact locations of cell initiation were simulated for a real case. Many simulated features at various scales were found to agree well with new (IHOP) and past observational data. Based on these simulations, a new conceptual model for dryline convective initiation was proposed. Other reviewer comments included: "The manuscript (Part I) nicely addresses some of the topics that IHOP hopes to answer including a better understanding of specific locations and timing of convection initiation"; and "This (Part II) is a great manuscript to go into the special issue volume for IHOP, since it is a nice modeling study that nicely supports what is being observed in the "real" data." Earlier, Geoffrey Stano, supervised by the PI, completed a M.S. degree analyzing the same case based on observations and high-resolution gridded analyses (Stano 2003).

The PI (Xue) used ARPS to produce very high-resolution (25 m) large (2000x2000x80) grid simulations of supercell storms, and obtained to date the most successful simulation of a tornado developing within an entire supercell storm (Xue 2004). The complete life cycle of an F5 tornado is simulated with surface winds exceeding  $120 \text{ ms}^{-1}$  and a central pressure drop of over 80 hPa. Multiple subvortices are resolved within the parent tornado. Detailed analyses on the data are being performed. The data set is also being used extensively for testing radar emulators and tornado detection algorithms within the CASA project. Ming Xue also published a paper on density current and squall line dynamics (Xue 2002). This data set has been extensively used within the NSF ERC CASA project for radar emulation and tornado analysis and detection studies (more details later).

Other refereed publications under the complete or partial support of this grant include: Shapiro et al. (2002; 2003) and Gao et al. (2004c) on single Doppler velocity retrieval, Gao et al. (2002; 2003; 2004a) on 3DVAR analysis of radar data and Gao et al. (2004) on a variational method for retrieving vertical wind profiles from radar data, Gao and Droegemeier (2004) on a variational velocity dealiasing algorithm, Brewster et al. (2003) on the assimilation of radar data for the detection of aviation weather hazards, Martin and Shapiro (2005) on the impact of radar tilt and ground clutter on clear-air wind measurements, Sharif et al. (2002; 2004) on radar error propagation in the fully coupled system, Chow et al. (2005) on a novel reconstruction model for subgrid-scale turbulence, Chow et al. (2006) and Weigel et al. (2006) on the simulations of steep-valley flows, Ren and Xue (2006) and Xue and Ren (2006) on 4DVAR retrieval of soil state variables, and Xu et al. (2006) on an error covariance model for wind analysis from radial velocity data. Dowell and Shapiro (2003) and Dabberdt et al. (2005) also acknowledge the support of this NSF grant. Complete PDF format files of most submitted manuscripts can be found at <http://twister.ou.edu/vita.html#pubs>.

### **3 Specific results**

Some of the results summarized in section 2 are presented in an expanded form in this section.

### **3.1 Real-time Forecast Support for IHOP 2002 and Precipitation verification of CAPS IHOP forecasts**

From May 13 through June 2002, the group successfully carried out real time forecast operations in support of IHOP field experiment using ADAS and ARPS. The effort leveraged on support from other related projects at CAPS. In addition to providing support for the real time operations of IHOP, we also had and successfully achieved the goals of obtaining an initial assessment of the forecast model performance during the period and of identifying specific data sets and cases for extensive retrospective studies. Some details of the real time forecast are given here.

The realtime forecasts were produced on three grids with 27, 9 and 3 km grid resolutions, respectively. The fine resolution grids were nested inside the coarser ones in one-way nested mode. These three grids cover the Continental US, the Central Great Plains, and the entire state of Oklahoma plus south-central Kansas and Texas panhandle, respectively (Fig. 1). These three grids are referred to as the US, SPmeso, and SPstorm grids, respectively.

The US and SPmeso forecast start from initial conditions (IC) at 12 UTC each day, and forecast for 42 and 24 hours, respectively (Fig. 2). Six-hour (06 UTC) NCEP Eta forecast fields were used as the analysis background, and the forecasts from the same Eta forecast cycle were used as the boundary conditions (BC) for the US grid. The SPmeso grid obtained its BC from the US grid. The 3 km SPstorm grid was run twice a day, starting at 15 UTC and 00 UTC. The 15 UTC SPstorm analysis used the 3-hour SPmeso forecast as the background, while the 00 UTC SPstorm forecast used 9-hour SPmeso forecast for its analysis background fields. Boundary conditions for both SPstorm forecasts were from the 12 UTC SPmeso forecast.

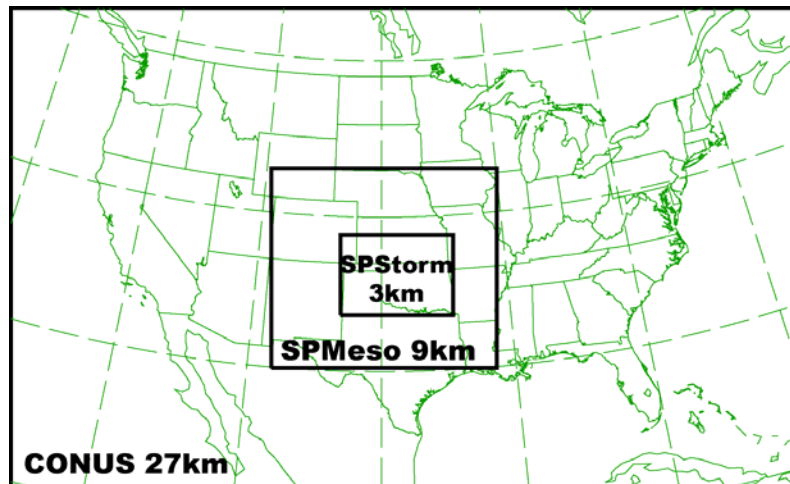


*Fig. 1. The 27, 9 and 3 km resolution ARPS forecast grids run during IHOP.*

The initial conditions were produced using the ARPS Data Analysis System. Data incorporated into the initial conditions included all available rawinsondes from the standard network and special launch soundings, wind profilers, standard surface observations, the Oklahoma and western Texas Mesonet data and DOE/ARM surface observations. A unique aspect of this work is the use of broadband, Level-II NEXRAD radar data from a network of radars through the Collaborative Radar Acquisition Field Test project.

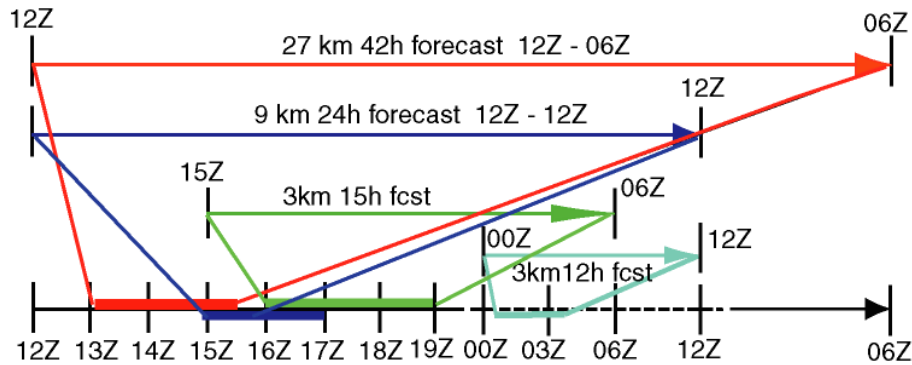


Fig. 2. Forecast timeline, showing the start and end times of forecasts, and wall clock times of the operations.

Level-II data from 12 radars and Level-III (NIDS) data from 12 others in the Central Great Plains were ingested in real-time, remapped to the ARPS Cartesian grids, and used in a cloud analysis procedure to improve the representation of water vapor, cloud water and other microphysical variables. The IC analysis includes a diabatic adjustment to modify the temperature field in the presence of cloud and vertical motion in the initial condition. Furthermore, where Level-II data were not available, the radar data from Level-III NIDS products were used. The cloud analysis also utilized visible and infrared channel data from GOES-8 satellite and surface observations of clouds. In addition to the forecasts performed at three resolutions, hourly analyses were produced on the SPmeso grid, making use of all of the data mentioned above.

To reduce the effect of imbalances in the initial condition, an incremental analysis update procedure was employed for the later part of the forecast period. This procedure is particularly effective for the 3 km forecast, where the analysis background was ARPS forecast. In this case, the analysis increment is introduced over a 10-minute period into the model, minimizing oscillations that can be introduced by imbalances in the analysis.

The number of horizontal grid points for the US, SPmeso and SPstorm grids were  $213 \times 131$ ,  $183 \times 163$  and  $273 \times 195$ , respectively, and all grids used 53 vertical levels with the model top being placed at 20 km above sea level. A full array of the ARPS physics package was employed. Recent improvements through validations against the Oklahoma Mesonet soil moisture measurements were incorporated into the soil model. A recently developed soil skin temperature initialization procedure that uses the Eta first guess field and the air temperature analysis was employed. The latest ARPS Version 5.0 was used.

The data ingest, preprocessing, analysis and boundary condition preparation were performed locally on three networked two-processor Pentium 4 Linux workstations. The model input data were then shipped to remote supercomputers at the Pittsburgh Supercomputing Center (PSC) or the National Center for Supercomputing Applications (NCSA). The three morning forecasts were run on one of the two Compaq Alpha-based clusters at PSC using 240 processors. The 00 UTC SPstorm forecast was run on NCSA's Intel Itanium-based Linux cluster, also using 240 processors. The model outputs were shipped back to local workstations and processed. Graphical products were posted on the Web. The entire operation was automated by a sophisticated Perl-based control system.

Graphical products, including fields and sounding animations, were generated and posted on the web as the hourly model outputs became available. A workstation dedicated to displaying

forecast products was placed at the IHOP operation center. As part of the real time CAPS support for IHOP, a CAPS scientist was on duty daily to evaluate and assist in the interpretation of the forecast products. A web-based evaluation form was used to provide an archive of forecast evaluations and other related information. The forecast products are available at <http://ihop.caps.ou.edu>, and will remain online throughout the length of our project to facilitate forecast evaluation and case studies. Initial results of our IHOP forecast experiment were reported at the 15th NWP Conference in August 2002 (Xue et al. 2002).

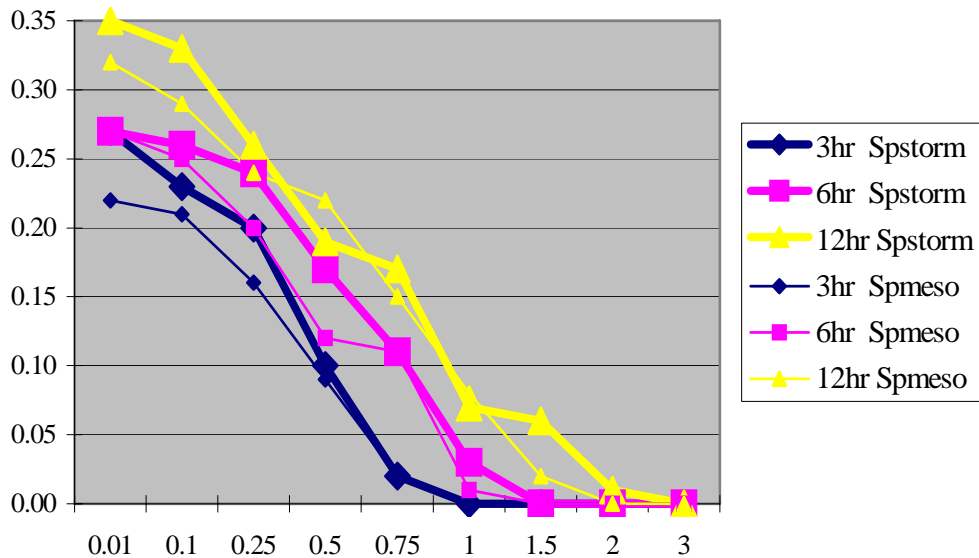


Fig. 3. Equitable threat score (ETS) of the 9km (SPmeso) and 3 km (SPstorm) CAPS IHOP forecasts verified against gauge data in the common 3 km forecast domain. It is clear that the 3 km grid (thick lines) consistently outperforms the 9 km grid (thin lines) for all three forecast ranges.

Working with M. Xue, visiting scientist Dr. J. Min developed a code and performed detailed precipitation verification studies of CAPS IHOP\_2002 real time forecasts on 27, 9 and 3 km grids against both NCEP Stage IV gridded and rainfall gauge data. Standard threat scores and Hövmöller diagrams were examined (Xue and Min 2003). The results were presented at the Spring IHOP Science meeting in Boulder CO in March 2003. Contrary to the findings of some other work, the results clearly show improved precipitation forecast skills as the grid resolution increases (Fig. 3). A complete re-run of IHOP forecasts is planned that will examine systematically the impact of cloud analysis using radar data on the precipitation forecast.

### 3.2 Phase-correction data assimilation technique and ARPS model and data assimilation system development

In 2003, K. Brewster published two papers (Brewster 2003a; Brewster 2003b) on a variational phase-correcting technique for storm-scale NWP. It was found that knowledge of phase errors determined from one variable in the dynamic system could be effectively used to

update the system, correct error in all the fields and improve the forward forecast of the system state. The technique was successfully applied to a three dimensional thunderstorm simulation.

Xue et al. (2003) documents the latest developments within the Advanced Regional Prediction System and presents results of applying high-frequency intermittent data assimilation that includes radar data to the prediction of a tornadic thunderstorm case. A new 3DVAR system developed for storm-scale data assimilation is also described together with a sample analysis.

### 3.3 Development of velocity analysis techniques from Doppler radar data

In Gao et al (2004b), the Gradient Velocity Azimuth Display (GVAD) and Gradient Volume Velocity Processing (GVVP) methods are developed for estimating the aerial mean vertical wind profile over a Doppler radar. The methods are much less susceptible to contamination by velocity ambiguities and noise in the data. The methods are tested first on idealized data to examine their sensitivity to different types of errors in radial velocity. It is found that the mean wind profiles retrieved using both methods are not sensitive to random errors in the radial velocities, even those with large amplitude. Tests of GVAD on a set of WSR-88D data collected during the 3 May, 1999 tornado outbreak show that it is capable of obtaining accurate wind profiles (Fig. 4) even when the raw data contain large errors caused by velocity ambiguities and random noise.

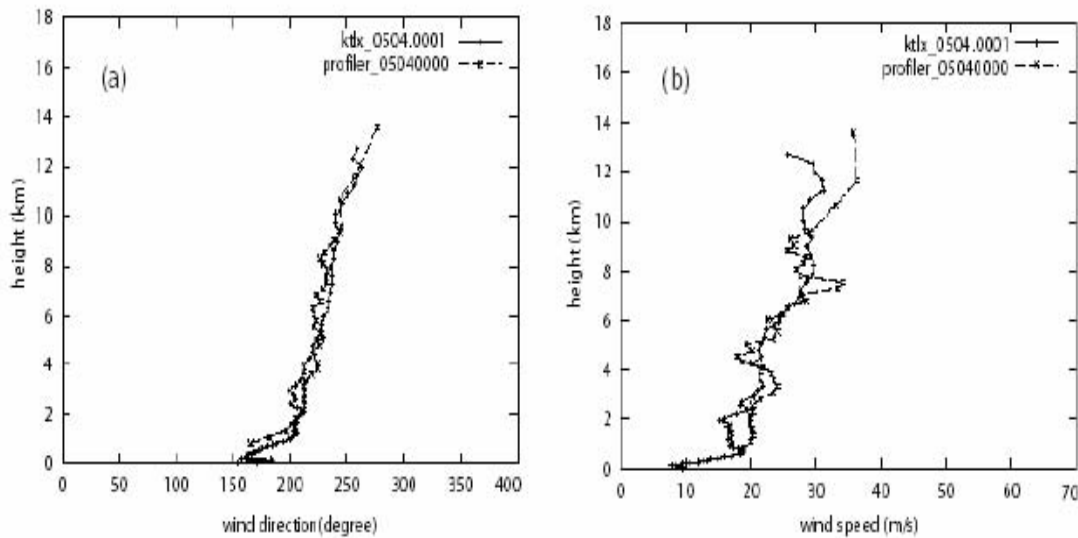


Fig. 4. Comparison of wind profile for 00 UTC of 4 May 1999 from wind profiler in Purcell, Oklahoma and that retrieved from KTLX radar using GVAD method for (a) wind direction and (b) wind speed.

### 3.4 Development of single-Doppler velocity retrieval techniques

In Shapiro et al (2003), an approximate (rapid-scan) dynamical model for single-Doppler retrieval of the vector wind field is investigated. This approximate model is based on the Lagrangian form of the radial component of the equation of motion, and is valid for retrieval time windows that are smaller than the effective time scale of the flow but larger than the

product of the effective time scale and (non-dimensional) relative error in the radial wind observations. The retrieval was tested with data gathered by two Doppler-On-Wheels mobile Doppler research radars of a cold front on 16 June 2000 near Grandfield, Oklahoma. Experiments focused on the sensitivity to time resolution of input data and the utility of a background constraint obtained from a VVP-like estimate of the wind field. Retrieval error statistics were substantially improved as the volume scan intervals decreased from 5 minutes (characterizing the current WSR-88D scan rates) down to 1 minute. Use of the background constraint also improved the results, with superior results obtained in the high temporal resolution experiments when the background constraint was selectively imposed.

### ***3.5 Development and testing of 3DVAR systems for Doppler radar assimilation***

In Gao et al. (2004a), a new method of Doppler radar wind analysis based on a 3DVAR approach is described. The 3DVAR system includes the mass continuity equation as a weak constraint and the background error covariance matrix is modeled using a recursive filter. The minimization problem is preconditioned by the square root of the background error covariance matrix. The method is applied to Doppler radar observations of a supercell storm and the analysis results are compared to a conceptual model and previous research. It is shown that the horizontal circulations, both within and around the storms, as well as the strong updraft and the associated downdraft, are well-analyzed. Because no explicit integration of the anelastic mass continuity equation is involved, error accumulation associated with such integration is avoided. As a result, the method is less sensitive to vertical boundary uncertainties. The system is also unique in that several scales of data can be accommodated using an iterative, scale telescoping approach. This 3DVAR system has proven quite effective as it has been used in more recent studies by our group (Gao et al. 2006c; Hu and Xue 2006; Hu et al. 2006a; Hu et al. 2006b).

### ***3.6 Data simulation and prediction of tornadic thunderstorms using level-II radar data with ARPS 3DVAR and cloud analysis***

The ARPS 3DVAR-cloud analysis combination has been shown to be efficient and effective through a number of case studies by our group for initializing convective storms (Hu et al. 2006a; Hu et al. 2006b). Typically, rapid update cycles at 5 to 15 minutes intervals are used. Hu and Xue (2006) examined various configurations of the intermittent 3DVAR-cloud analysis data assimilation procedure for the 8 May 2003 Oklahoma City tornadic thunderstorm case, using a nested 3 km grid. Forecasts for up to 2.5 hours were made from the assimilated initial conditions. For the case, it was found that one-hour long assimilation window covering the entire initiation stage of the storm worked best. The results also show that when the data from a single Doppler radar is assimilated with properly chosen assimilation configurations, the model is able to predict the evolution of the 8 May 2003 Oklahoma City tornadic thunderstorm rather accurately for up to 2.5 hours. In Hu (2005), even better results were obtained using a 1 km grid. The prediction captured well the hook echo structure and radial velocity couplets associated with the observed tornado; they compared well against low-elevation radar observations. When a 100 m grid was further nested within the 1 km grid, an F2-intensity tornado was obtained in the model prediction (Fig. 5 and Fig. 6), whose predicted track was less than 5 km from the observed tornado track. This is, we believe, the first time ever that a tornado is predicted by a numerical model that was initialized using real data, including those of radar.

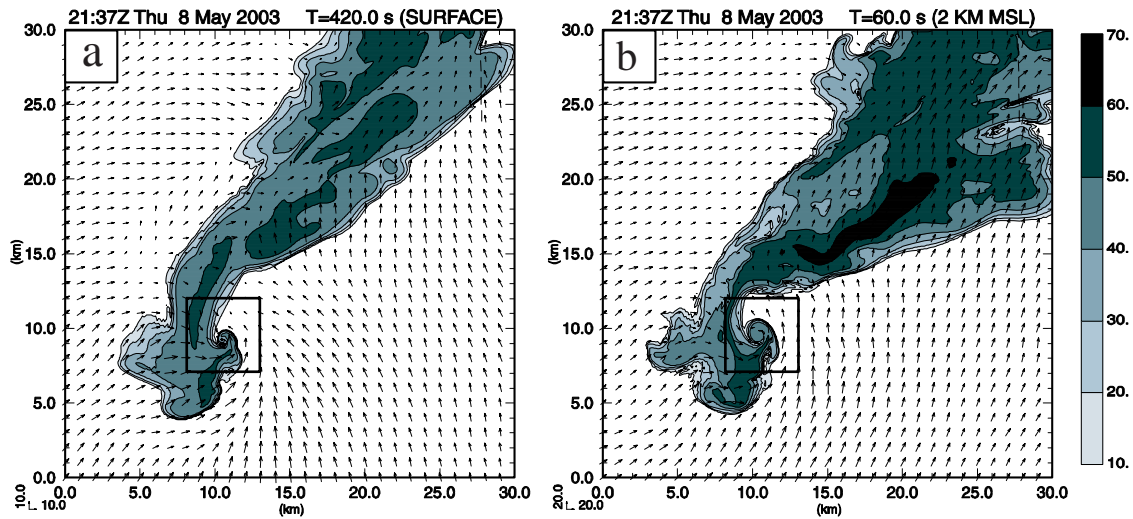


Fig. 5 Predicted reflectivity and wind fields at the surface (left) and 2 km MSL (right) from at 7 minutes into the 100 m forecast. The square in the figures indicates a zoomed-in area to be shown in next figure. Wind vectors are plotted every 10 grid points. The presence of a tornado is indicated by the hook echo that contains reflectivity spirals into the circulation center.

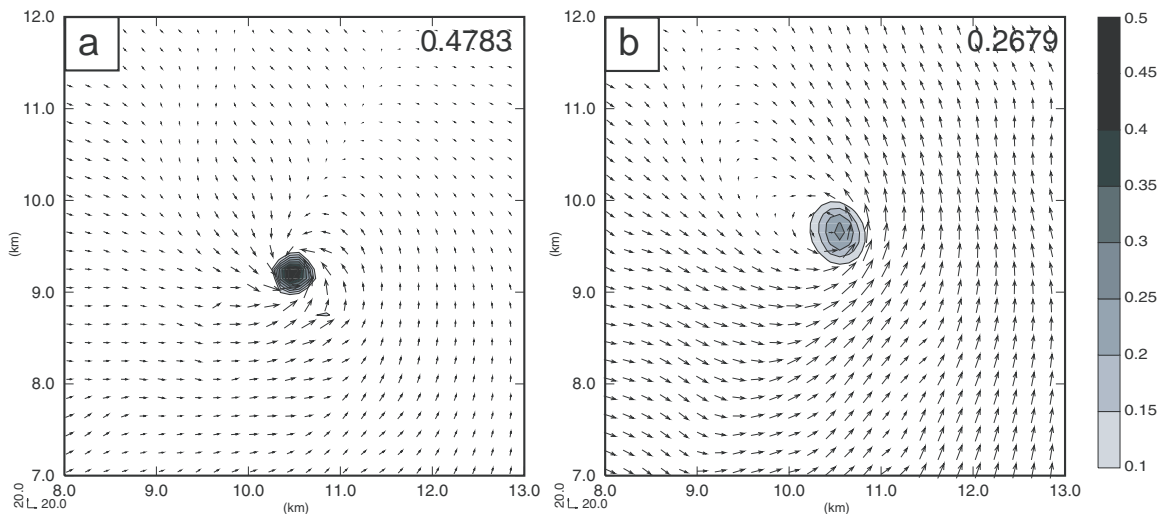


Fig. 6. Predicted wind and vertical vorticity fields at the surface (left column) and 2 km MSL (right column) from 7 minute forecast valid at 2137 UTC. The domain corresponds to the square box found in Fig. 5. The numbers at the upper-right corner are the maximum vertical vorticity value in  $s^{-1}$ .

### 3.7 3DVAR analysis of water vapor field from GPS slant-path and surface network data

Ph.D. student, H. Liu, developed a 3D variational (3DVAR) system for analyzing the three-dimensional water vapor structure from GPS slant-path water observations. A set of Observing Simulation System experiments (OSSEs) were completed. The ARPS mesoscale model was used

to produce a detailed 3D atmospheric moisture field for an IHOP 2002 case containing a dryline, and this was used as truth for the OSSEs. The system uses explicit or recursive spatial filters to model flow-dependent background error covariances and is formulated in terrain following coordinates. The results of the OSSEs illustrate that this variational retrieval method can properly recover mesoscale three-dimensional moisture structure and accurately capture major features of water vapor field simulated by the model including surface observations (Liu and Xue 2004, 2006a; Liu et al. 2006a). In addition, sensitivity experiments were conducted to test the addition of surface moisture observations to the OSSE and a vertical filter on the retrieval. Fig. 7 shows results from Liu et al. (2006a) comparing the moisture analyses for a dryline case from simulated slant-path water vapor data, using an isotropic recursive filter (IRF) (Fig. 7a) and a flow-dependent anisotropic recursive filter (ARF, Fig. 7b). The correlation coefficients with the truth for the analysis increments using IRF and ARF are 0.83 and 0.93, respectively, similar to the results of Liu and Xue (2006a) using explicit filters. The figure shows clearly that the anisotropic formulations outperform the isotropic ones.

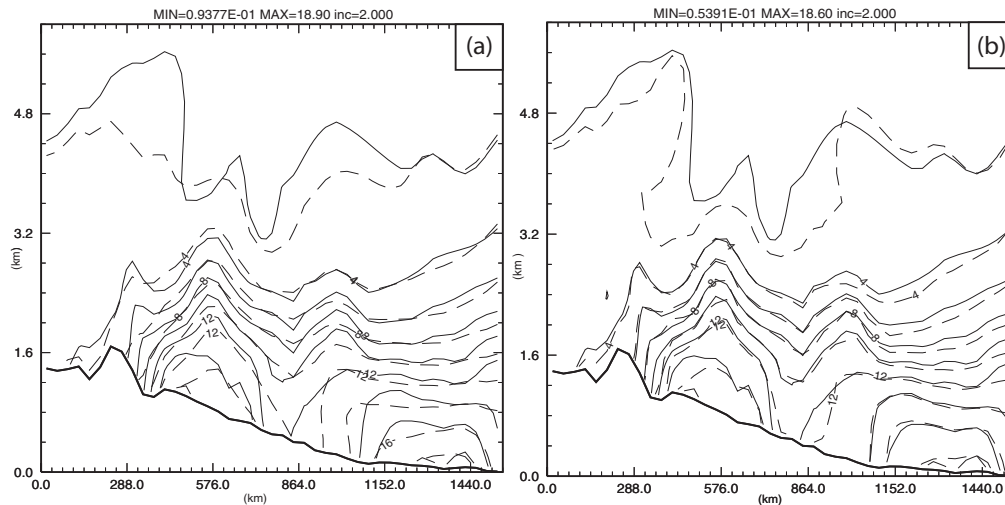


Fig. 7. East-west cross-section of specific humidity field through a simulated dryline from IHOP\_2002, as analyzed using 3DVAR (dashed lines) with (a) an isotropic spatial filter and (b) an anisotropic filter, as compared with the truth in solid lines.

### 3.8 High-resolution modeling studies on dryline convective initiation for IHOP cases

Masters student G. Stano performed an observation-based analysis of the convective initiation processes in the 24 May 2002 case observed during the IHOP field experiment (Stano 2003). At 2000 UTC on 24 May 2002, a strong line of storms developed in the Texas panhandle area and moved across the state of Oklahoma and northern Texas. The study investigated the causes for convective initiation on 24 May 2002 using gridded fields produced by the ARPS Data Analysis System (ADAS) as well as by examining raw observations. Special IHOP data sets, including those from regional and mobile surface and upper-air networks, and those from many remote sensing platforms, were used in the objective analysis. It was shown that the initial storms developed due to the interaction of the surface cold front and the dryline. The initiation region was favored over locations further to the northeast along the surface cold front due to

strong surface heating, a weakening of the stable layer above the boundary layer, and by more effective upper-level support.

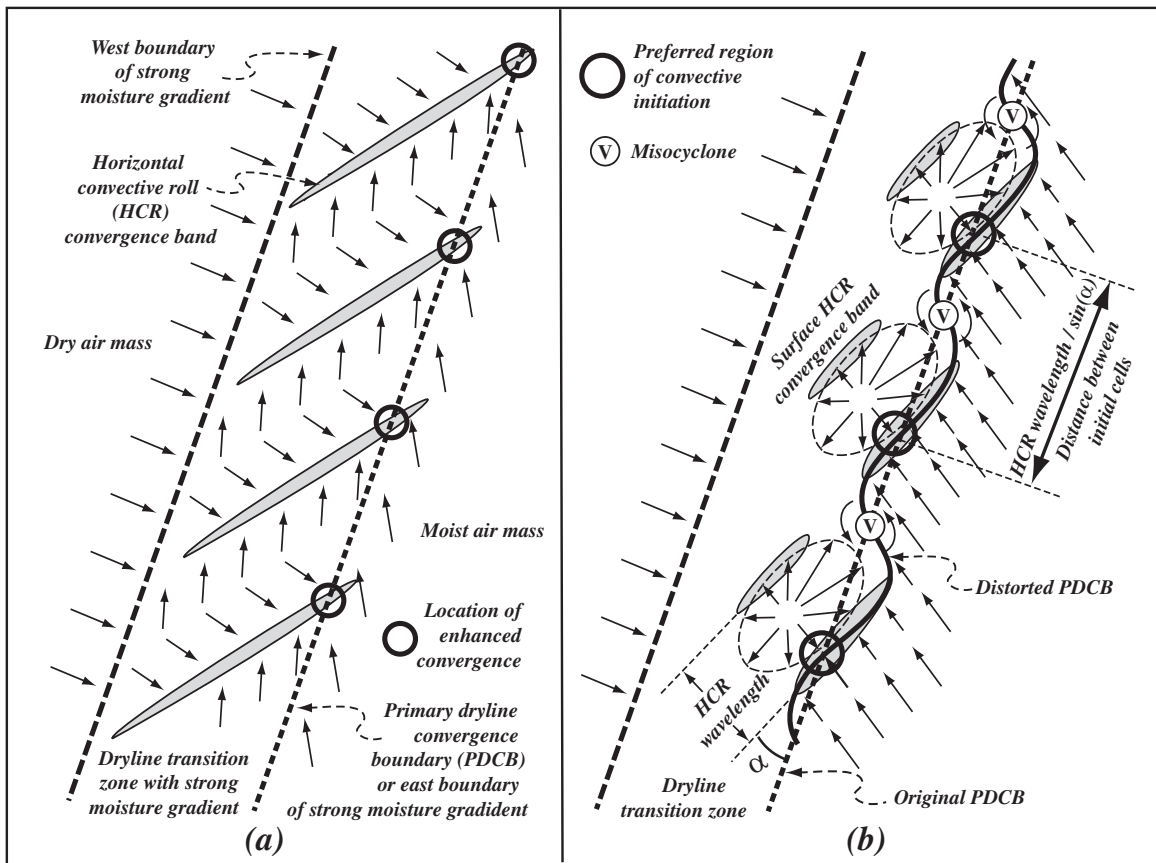


Fig. 8. A conceptual model of dryline convective initiation due to the interaction of the primary dryline convergence boundary (PDCB) with the evolving horizontal convective rolls (HCRs) that originate at and on the west side of the PDCB and are aligned at an acute angle,  $\alpha$ , with the dryline. The PDCB is the boundary between the southerly to southeasterly moist flow, and the drier generally westerly flow in the dryline transition zone, where a strong moist gradient is found. The PDCB undistorted by the HCR circulation is marked by the thick, straight, short-dashed line. The thick, straight, long-dashed line marks the location of the western boundary of the dryline transition zone, toward the west of which the air is exclusively from the dry high plateau to the west with a specific humidity of few grams per kilogram. Panel (a) shows the earlier stage of HCR development when the HCRs are quasi-two-dimensional and the roll circulations result in surface divergence flow and convergence bands (shaded gray) between the opposing roll circulations. The background southwesterly wind in the transition zone causes the surface divergence flow of the rolls to point in the downwind direction. The rolls are aligned in the direction of the mean low-level vertical shear vector and the northeastern ends of the convergence bands intersect the PDCB, creating localized convergence maxima. Panel (b) shows the low-level flow at the mature stage of HCR development, about 1-2 hours after panel (a), when significant cellular structures develop with the rolls

*and the convergence bands becoming segmented and shorter but more intense. The convergence bands protrude further into the moist air mass across the original PDCB and distort the PDCB into a wavy pattern. The divergence flow between the convergence bands develops into asymmetric elliptic patterns, with the northeastward wind components being stronger due to downward transport of southwesterly momentum and due to the original background flow in the same direction. The mesoscale convergence along the dryline is enhanced by the elevated heating to the west hence by the increased solenoidal forcing. It narrows the dryline transition zone, turns the HCRs into a more north-south orientation. The easterly component of the moist flow is increased, which, together with HCR divergence flow, creates convergence maxima along the PDCB, at locations marked by thick circles, where convective initiation is preferred. Such locations are also roughly where HCRs intersect the original PDCB and the distance between such preferred locations is roughly equal to the HCR wavelength divided by  $\sin(\alpha)$ . When the initiated clouds move along the HCR convergence bands, they develop into deeper clouds faster and have a much better chance of growing into a full intensity convective storm. When older cells that are initiated at the persistent maximum low-level convergence forcing move away, new cells tend to form at the same location, resulting in a series of cells. The thin circles enclosing 'V' indicate locations of vorticity maxima (or misocyclones) along the PDCB. Misocyclones usually do not co-locate with maximum surface convergence but their circulation can enhance convergence to their south and north, and non-supercell tornadoes can develop when their vertical vorticity is stretched by cumulus congestus clouds that move over them.*

In Xue and Martin (2006b; 2006a), a successful simulation of the 24 May 2002 case is described. The ARPS model is used to simulate the evolution of the dryline and the intersecting cold front as well as the initiation and development of convective storms along and near the dryline and cold front. Using a large (700 km  $\times$  400 km) 1 km horizontal resolution grid nested within an even larger 3 km grid, the model is able to accurately predict the evolution of the dryline, the development and evolution of realistic boundary layer convective eddies and horizontal rolls, and most importantly, the timing and location of convective initiation along a section of dryline in western Texas. The model predicted the timing and location of convective initiation accurate to within 20 minutes and 25 km, respectively.

In Xue and Martin (2006b), it is suggested that the interaction between the dryline and the horizontal convective rolls from the west side of the dryline play an important role in determining the preferred locations of convective initiation along the dryline. Such interaction creates surface convergence maxima that provide additional forcing to lift air parcels above their level of free convection (LFC). The mesoscale convergence in the dryline zone and the resultant upward bulging of the well-mixed moist boundary layer created a favorable zone for moist convection. In Xue and Martin (2006a), the development and evolution of the boundary layer (BL) horizontal convective rolls (HCRs), and open convective cells (OCCs) and their interaction with the dryline are analyzed in detail. The processes by which a series of (moist) convective cells are triggered and the possible role of misocyclone vortices that form along the main convergence line are analyzed in detail. A new conceptual model that summarizes our findings is proposed and is shown in Fig. 8.

### 3.9 Data impact studies for IHOP cases

Masters student D. Dawson conducted a set of large domain, high-resolution experiments with the 15 June 2002 bow echo/MCS case. The forecasts are designed to investigate the impact of mesoscale and convective-scale data on the initialization and prediction of an organized convective system. Specifically, the forecasts test the impact of special mesoscale surface and upper-air data collected by, but not necessarily specific to, the IHOP project and of Level-II data from multiple WSR-88D radars. The effectiveness of using 30-minute assimilation cycles with the use of a complex cloud analysis procedure and high temporal-resolution surface data is also examined.

The analyses and forecasts employ doubly-nested grids, with resolutions of 9 and 3 km. Emphasis is placed on the solutions using the 3 km grid. In all forecasts, a strong, well-defined bow-shaped MCS is produced with structure and behavior similar to those of the observed system. Verification of these forecasts through both regular and phase-shifted equitable threat scores of the instantaneous composite reflectivity fields indicate that the use of the complex cloud analysis has the greatest positive impact on the prediction of the MCS, primarily by removing the otherwise needed “spin-up” time of convection in the model. The impact of additional data networks is smaller, and is reflected mainly in reducing the spin-up time of the MCS. The use of intermittent assimilation cycles appears to be quite beneficial when the assimilation window covers a time period when the MCS is present. Difficulties with verifying weather systems with high spatial and temporal intermittency are also addressed, and it is found that the use of both regular and spatially-shifted equitable threat scores is very beneficial in assessing the quality of the forecasts.

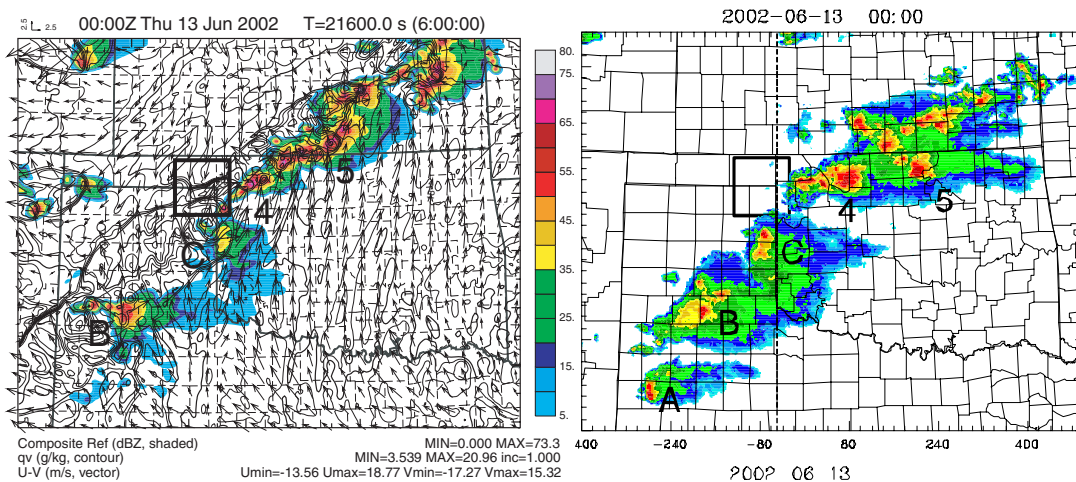


Fig. 9. Left: The forecast surface water vapor mixing ratio (contours,  $\text{g kg}^{-1}$ ), the wind vector ( $\text{m s}^{-1}$ ) and composite reflectivity (shaded, dBZ) at 0000 UTC, 13 June, 2002. Right: The observed low-level reflectivity field valid at the same time. The capital letters and bold numbers indicate the locations of primary convective cells.

Data impact studies have also been performed for other IHOP case. Results for the 24 May 2002 dryline convective initiation case from IHOP\_2002 field experiment were published in Xue and Martin (2006b; 2006a), while newer results on the 12-13 June 2002 convective initiation

case are excellent and are summarized in Liu and Xue (2006b) and Xue and Liu (2006). Fig. 9 compares with radar observations the 6-hour ARPS forecast of convective cells initiated along a dryline and a thunderstorm outflow boundary, in which special data collected by IHOP were assimilated hourly over a 6-hour period. The 3 km and 1 km grids used had about 300x800 and 860x700 grid points in the horizontal, respectively.

### 3.10 Impact of lateral boundary conditions on ensemble forecasts

Working with Drs. M. Xue and D. Stensrud, P. Nutter completed his Ph.D. dissertation (Nutter 2003) and published two papers (Nutter et al. 2004a; Nutter et al. 2004c), examining the effect of lateral boundary conditions (LBCs) on limited-area ensemble forecasts. Through a set of carefully designed nested ensemble forecast experiments, the specific effects of the lack of fine-scale structures and/or high-frequency signals in the LBCs on the error growth and dispersion of nested limited-area ensemble forecasts were clearly documented. A new method was developed to apply statistically consistent LBC perturbations at each time step that remain spatially and temporally coherent while passing through the boundaries. It was shown that the LBC perturbations could capably restore error variance growth and LAM ensemble dispersion without compromising the integrity of the individual solutions.

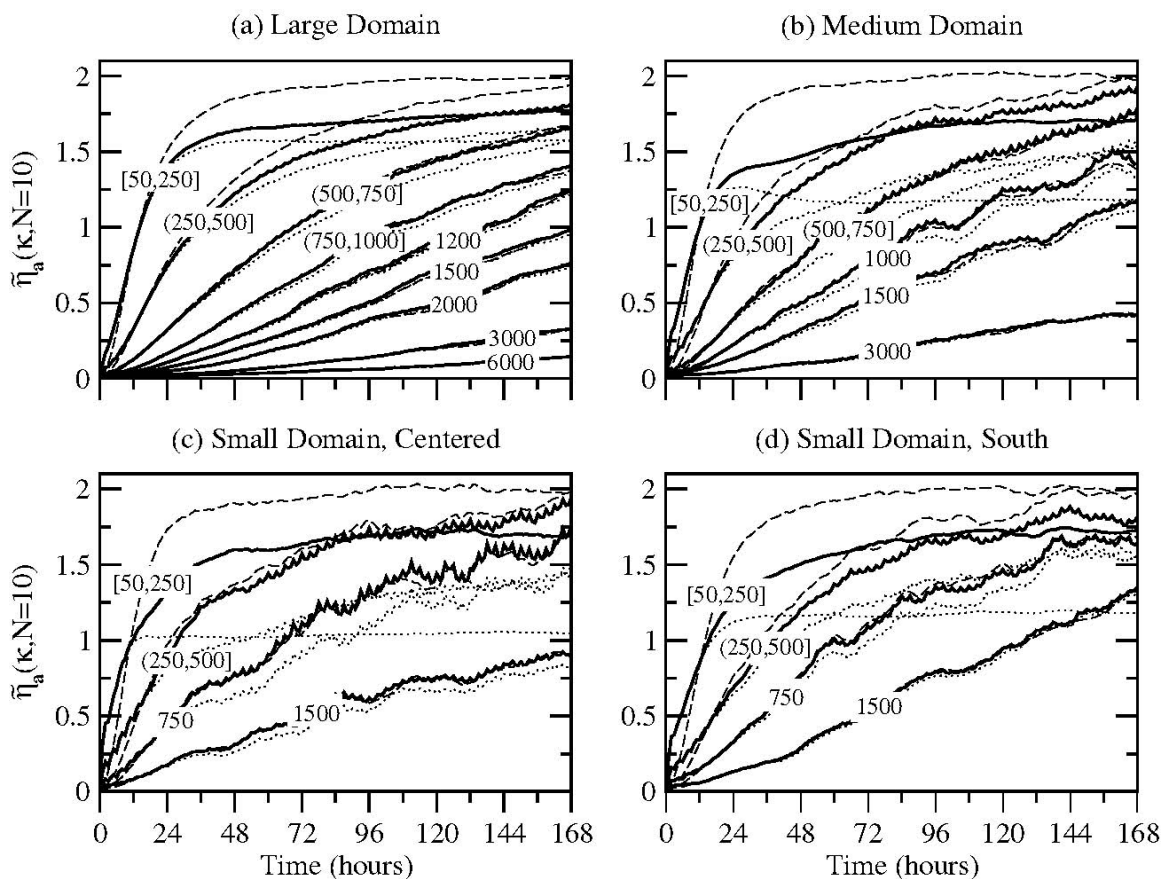


Fig. 10. Normalized vorticity error variance, averaged over 100 independent 10-member LAM ensemble simulations having perturbed 3hourly updated, low-pass filtered LBCs (150 km wavelength cutoff). Line labels (km) indicate wavelengths

*contributing to error variances. Dashed reference lines show error variances from subsets of global ensemble simulations and dotted lines show error variances from corresponding LAM ensemble simulations run without LBC perturbations.*

Fig. 10 shows that the application of LBC perturbations completely restores error variances at wavelengths longer than about 500 km to values obtained from control simulations run on the global domain. The LBC perturbations are less effective for smaller scales, where the proportion of error variance restored depends on domain size. For example, on the large domain (Fig. 10a), the LBC perturbations restore about 1/3 of the error variance lost at saturation in the smallest scales. Compare this to the small, centered domain (Fig. 10c), where the LBC perturbations restore more than 3/4 of the error variance lost in the unperturbed LAM simulations.

### **3.11 Ensemble Kalman filter data assimilation**

Ph.D. student, M. Tong, with initial contributions from W. Martin, developed an ensemble Kalman filter (EnKF) system based on a compressible model, the ARPS, and applied it to the assimilation of radar radial velocity and/or reflectivity data at the convective scale (Tong and Xue 2004, 2005b; Tong 2006). Based on a set of OSS experiments, it was shown that not only can the wind and thermodynamic fields be retrieved accurately, but all five categories of hydrometeors employed by the ice microphysics scheme can also be successfully retrieved. Fig. 11 shows two examples of assimilation experiments in which radial velocity of different spatial coverage were assimilated.

In Xue et al (2006a), the ARPS EnKF data assimilation system is used to study the effectiveness and impact of data from a network of four low-cost radars planned (at that time, now deployed) for the Oklahoma test-bed of CASA. The benefit of having these radars providing low-level coverage missing from NEXRAD is clearly demonstrated. In Tong and Xue (2006b; 2006a), the EnKF method is for the first time successfully applied to simultaneous estimation of the atmospheric state and parameters in an ice microphysics scheme. A new project involving EnKF is the assimilation of polarimetric Doppler radar data and initial results with simulated data are encouraging (Jung et al. 2006). Godfrey et al. (2005) applied the EnKF method to further study the impact of CASA radar data and scanning strategies on the analysis and prediction of storms of different types. Gao and Xue (2006a; 2006b) developed a new efficient multi-resolution EnKF data assimilation algorithm. By combining a single high-resolution analysis and prediction cycle and a lower-resolution ensemble, computational cost of performing ensemble EnKF data assimilation is significantly reduced without too much sacrifice in the quality of analysis and forecast (Gao and Xue 2006a).

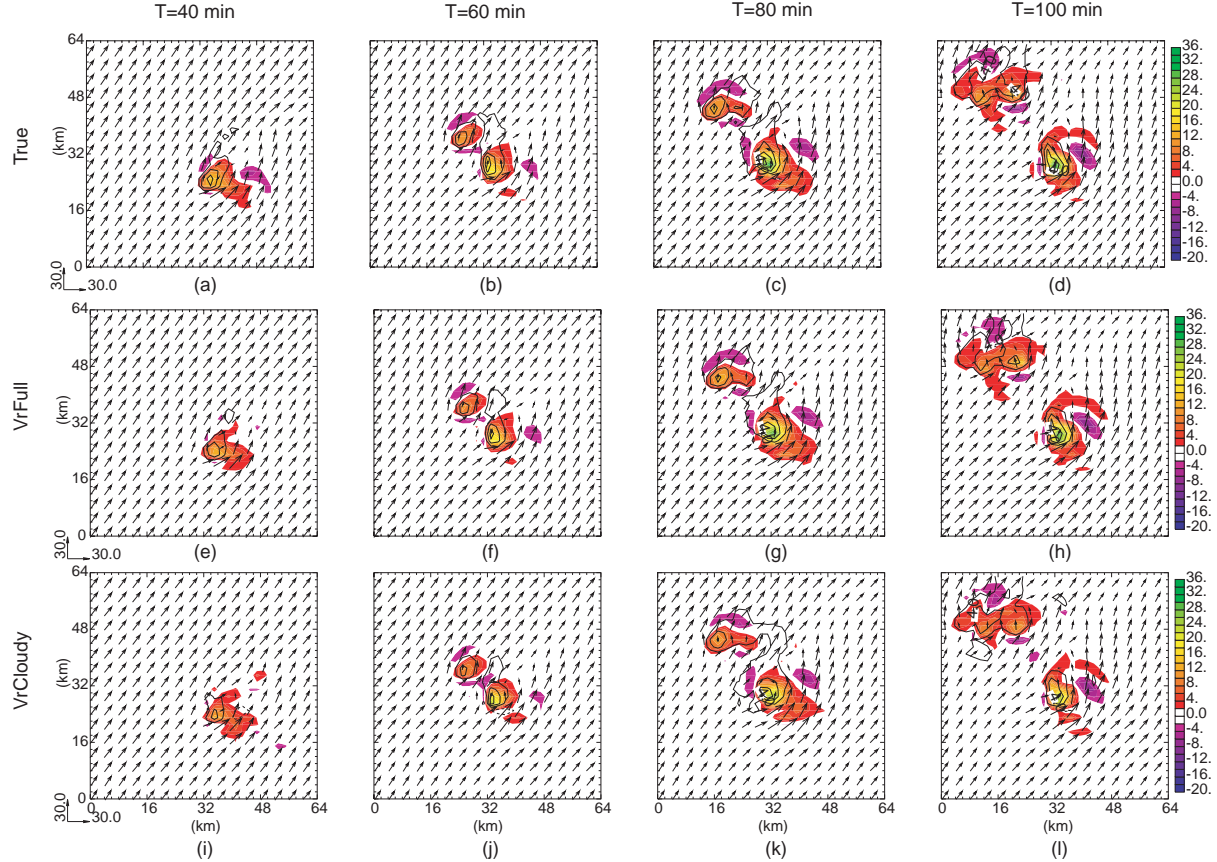
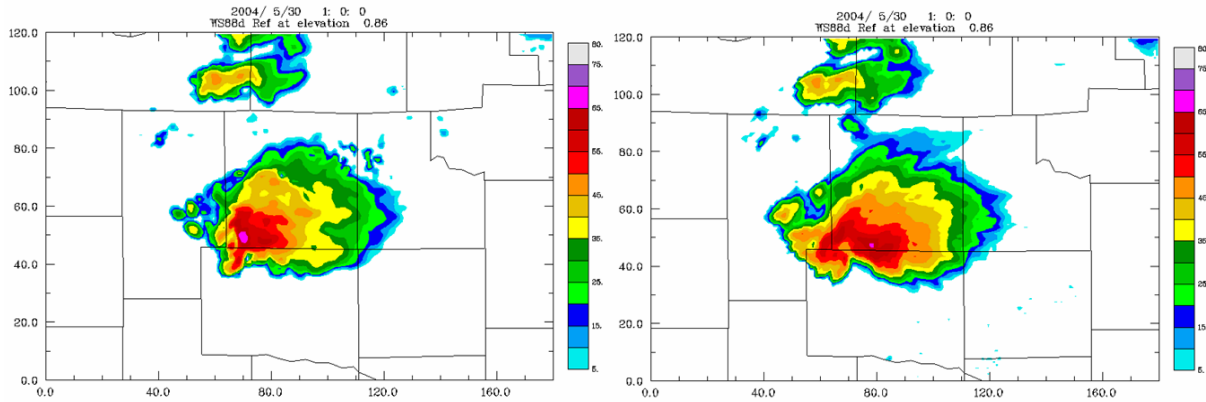


Fig. 11. Vertical velocity ( $ms^{-1}$ , shaded), horizontal wind vectors ( $ms^{-1}$ ), and perturbation potential temperature  $\theta'$  (K, contours) at  $z=6$  km for truth simulation (a)-(d), assimilation experiment VrFull that assumed radial velocity is available in the entire domain (e)-(h); and for VrCloudy that assumes radial velocity data are available when reflectivity is larger than 10 dBZ (i)-(l); at  $T=40, 60, 80$  and  $100$  min for a supercell storm. Assimilation of radial velocity data started at 25 mins.

Studies with EnKF and real data are so far very limited. With real data, the presence of model error poses many more challenges not faced when assimilating simulated data using a perfect model. Within M. Tong's Ph.D. study (Tong 2006), she applied our EnKF system to the May 29-30, 2004 northern Oklahoma City tornado thunderstorm case (Xue et al. 2005a). The radial velocity and reflectivity data from Oklahoma City WSR-88D (KTLX) and/or Enid, OK (KVNK) radars were assimilated. The assimilation used a  $180 \times 120$  km grid at 1 km resolution, and 40 ensemble members. The results are rather encouraging. Fig. 12 shows the analyzed reflectivity at the end of a 1-hour assimilation period, interpolated to the  $0.86^\circ$  elevation of KTLX radar (left panel), as compared to the observation (right panel). The analyzed storm exhibits typical supercell structures, including low-level hook echo, mid-level mesocyclone, intense updraft, as well as low-level gust front and convergence center (not shown). Some discrepancies between the analysis and observation are also evident, and divergence of the model forecast from observation is found in the ensuing forecast, suggesting imperfect analysis and/or the presence of significant model error. Work continues in improving the general EnKF assimilation algorithms and evaluating the impacts of various sources of errors.



*Fig. 12. The analyzed reflectivity field at the 0.86° elevation (left) as compared to the corresponding observed reflectivity (right), at the end of a hour-long assimilation period, for the May 29-30 2004 north Oklahoma City tornadic thunderstorm. OKC WSR-88D radar radial velocity and reflectivity data were assimilated.*

### **3.12 High-resolution simulations of tornadoes with a supercell storm and the use of the data for OSSEs (Observing System Simulation Experiments)**

The PI of the grant, Ming Xue, using the ARPS model and supercomputing facilities at the Pittsburgh Supercomputer Center (PSC), recently obtained the most-intense tornado ever simulated within a realistic supercell storm. The highest resolution simulations used a resolution of 25 m in the horizontal 20 m in the vertical at the ground level (which increases gradually with height). The simulation used a horizontally uniform grid covering a 48x48 km domain, with the model top located at 16 km above ground. The use of a uniform resolution grid large enough to contain the entire parent storm is a first, and eliminates the uncertainties of artificial human control associated with nested grid simulations or simulations using horizontally stretched grids. In fact, the most intense tornado that developed in these simulations did so at an unexpected location within the model domain. Fig. 13 plots the time series of domain-wide maximum ground-relative surface winds and minimum perturbation pressure, showing the peak wind speed reaching  $120 \text{ ms}^{-1}$  (which occurred at about 30 m above ground), and a pressure drop of over 80 mb. The peak wind speed places the tornado within the F5 intensity scale of Fujita. This set of simulations used 2048 Alpha processors on the Terascale computing facility at PSC. Each hour of model simulation requires 24 hours of wall clock time, and produces 3 terabytes of 16-bit compressed output of the 3D volume data, at 5 second intervals.

Fig. 14 shows the horizontal wind vectors and model simulated reflectivity in a subdomain depicting low-level circulations and a hook of reflectivity spiraling into the center of a tornado. Worth noting is that this particular tornado formed behind the surface gust front and within the cold pool, which is depicted by the gray shaded negative temperature perturbations in the entire domain plotted. Fig. 15 is a close-up view of the low-level circulation, reflectivity and the cold pool, at the time when tight low-level circulation first developed. Fig. 16 shows a 3D visualization of the simulated tornado, that exhibits a condensation funnel reaching the ground

containing intense rotation. The figure also shows significant changes in flow in the lowest 1 km of depth.

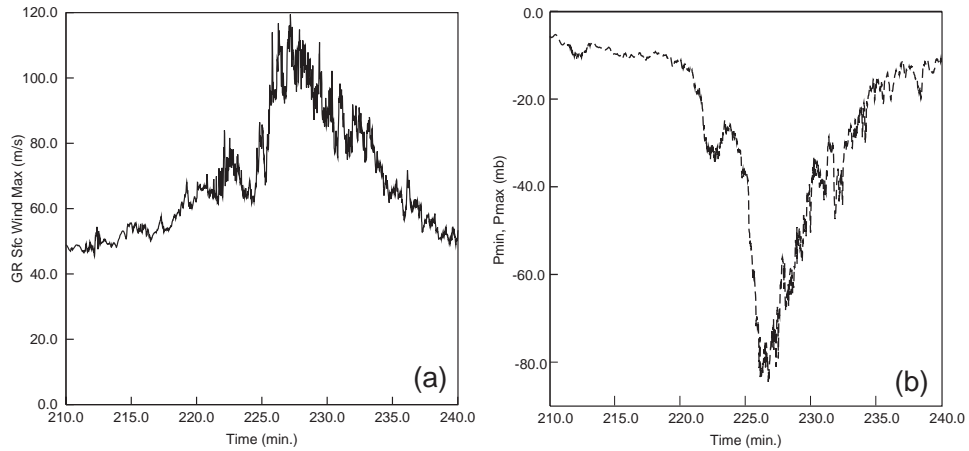


Fig. 13. Domain wide maximum ground relative surface wind speed (a) and minimum pressure perturbation (b) spanning the model intense tornado obtained in the 25m-resolution simulation.

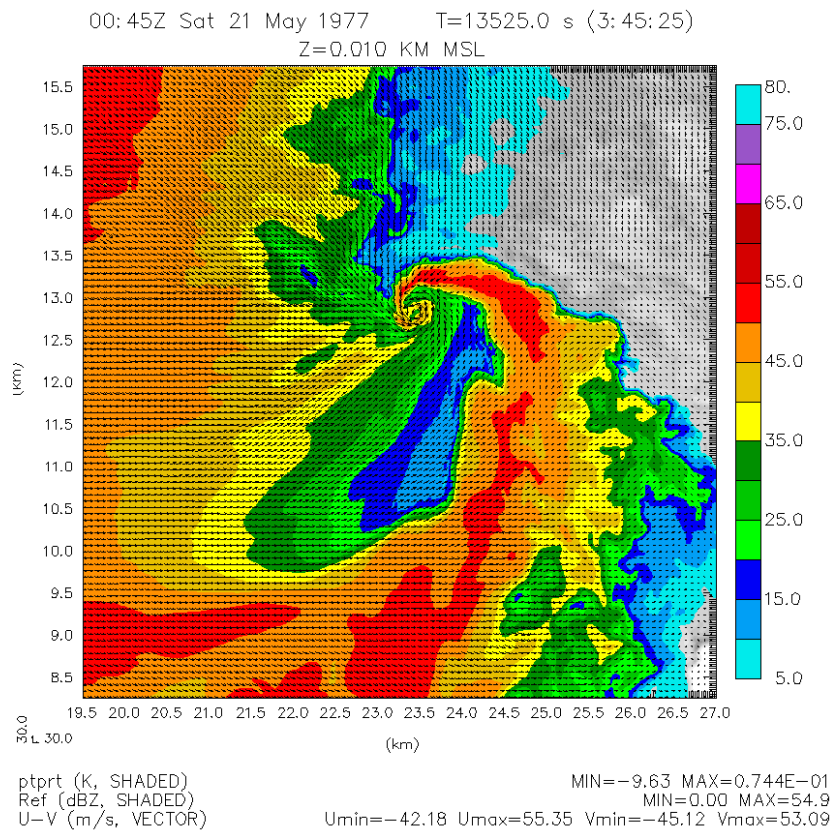


Fig. 14. Horizontal wind vectors and model simulated reflectivity (color) and perturbation potential temperature (gray shading) at 10m above ground.

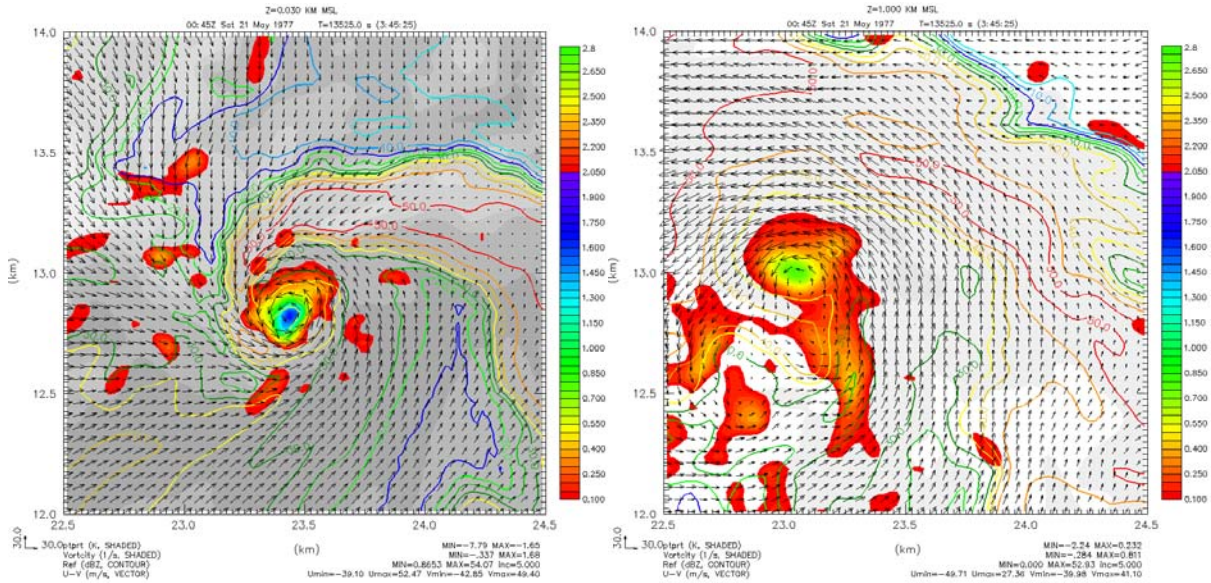


Fig. 15. Wind flow (vectors), reflectivity (colored coded contours), and perturbation potential temperature (gray shading), at 30 m AGL (the level at which the wind was strongest, left panel) and at 1 km AGL (right panel). The winds are relative to the model grid which is moving at a speed of about  $15 \text{ ms}^{-1}$  in a north-northeast direction and the fields have been smoothed twice to improve legibility.

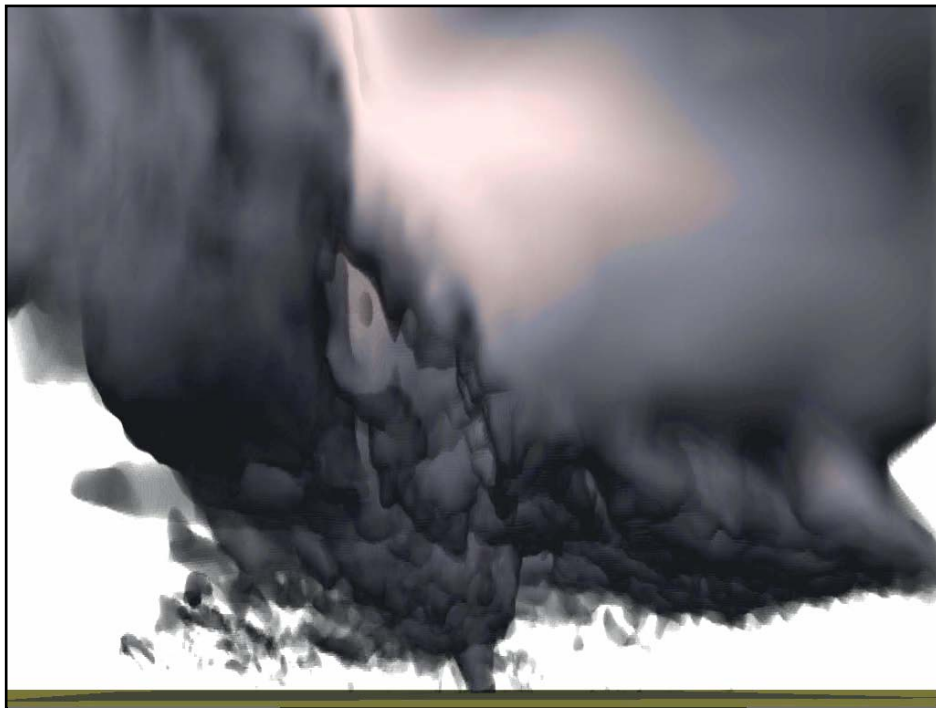


Fig. 16. 3-D visualization of the model simulated cloud water field depicting a tornado condensation funnel. Other realistic features include a lowered wall cloud (lower right), and a very low cloud base surrounding the tornado. The

*domain shown is 7.5 km wide and about 2 km deep (Greg Foss of Pittsburgh Supercomputing Center worked with the PI in creating this visualization).*

During the model simulations, which spanned more than 4 hours, many other vortices developed in the storm system, some with the intensity of weak tornadoes. These simulations provide valuable high-resolution data sets for performing OSSE experiments in the NSF ERC CASA project that test radar sampling strategies, radar network design, tornado detection algorithms, signal attenuation, among other things (Lyons et al. 2005; Liu et al. 2006b; May et al. 2006; Potvin et al. 2006; Xue et al. 2006b).

### ***3.13 Initial Condition Sensitivity Study Using Very Large Ensembles***

In Martin and Xue (2006c), sensitivity analyses were done using very large (several thousand member) ensembles of forward model runs that perturb the initial model fields one small patch at a time, so that sensitivity maps of the subsequent forecast fields (e.g. precipitation) to the initial condition (different variables at different regions) can be calculated. For example, sensitivity fields of the forecast precipitation to the initial low-level moisture were constructed. Some strong nonlinear sensitivity was found near the cold front. In one case, a  $1 \text{ g kg}^{-1}$  perturbation at the lowest 1 km depth over a  $27 \times 27 \text{ km}^2$  area triggered an entire new storm along the cold front (Fig. 17), a sensitivity that is larger than what has been documented in the literature.

This above work has been extended more recently with new approaches that require fewer ensemble members (Martin and Xue 2006b; 2006a). In this study, a large number (~2000) of forward model runs with randomly perturbed initial fields are made and the correlation (or sensitivity) between forecast quantities and initial fields are calculated statistically. Similar methods are used in the calculation of covariances between variables at the forecast time as part of ensemble Kalman filter (EnKF) schemes which typically use 10 to 100 members. However, the calculation of sensitivities (or covariances) between a forecast quantity and model fields at an earlier time is typically much noisier than the calculation of covariances between quantities at the same time. Consequently, a much larger (than typically used) ensemble size was found to be necessary. The results thus obtained, however, are excellent, as the technique is found to accurately calculate three-dimensional initial condition sensitivity fields without the need for linearizing the model (as is required by an adjoint) or simplifying the microphysics. The new method is much more efficient than that of the earlier method of Martin and Xue (2006c). Fig. 18 shows (a) the correlation coefficient between the total rain that fell in the indicated box, to the boundary layer water vapor field three hours earlier, and (b) the same field in a vertical cross-section.

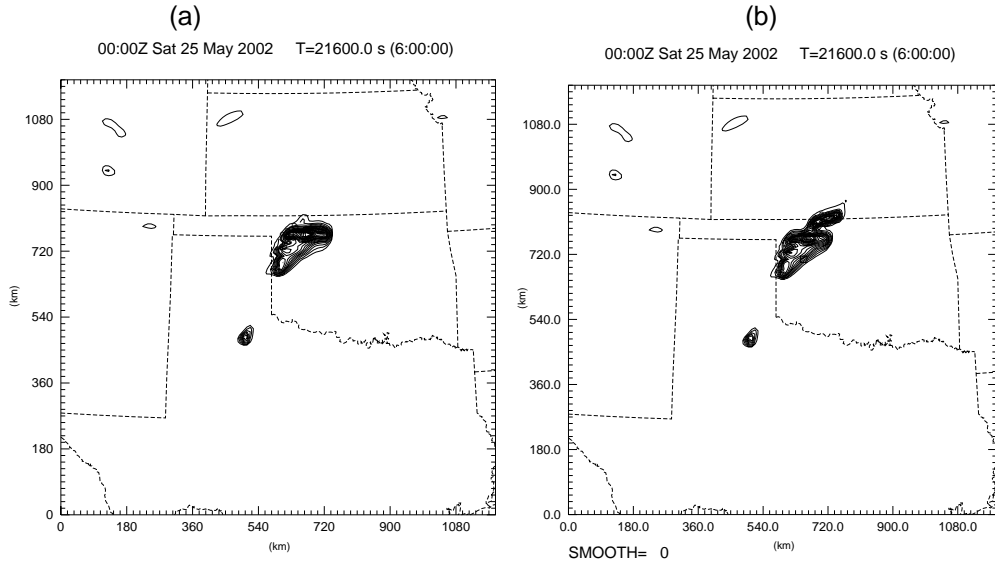


Fig. 17. Six-hour forecast of accumulated precipitation from control run (a) and from a model run with an initial  $1 \text{ g kg}^{-1}$  surface moisture perturbation at the location indicated by a small box in northwest Oklahoma (b). The extra local maximum in the precipitation along the Kansas-Oklahoma border of the perturbed run (b) is 120 mm.

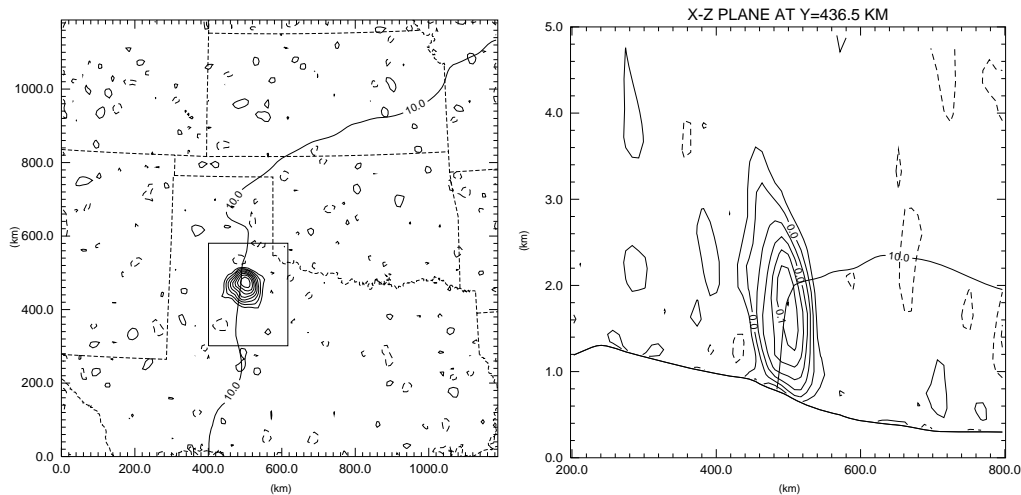


Fig. 18. Correlation coefficient between the rain which fell in the box drawn in (left panel) to the initial boundary-layer water vapor field (left panel) and (right panel) same field but in vertical cross-section along an east-west line through the area of large correlation coefficient in the left panel.

### 3.14 Development of the adjoint of a complete nonhydrostatic model for sensitivity and data assimilation studies

To perform the proposed adjoint sensitivity experiments, a new version of the adjoint code based on the latest version of the ARPS was developed (Xiao et al. 2005). This was being

done with the help of an automatic adjoint code generator, TAF which is the commercial version of the popular TAMC program (Tangent-linear and Adjoint Model Compiler). Some funds from this project were used to purchase the license for the TAF software. So far, the full-physics ARPS adjoint, except for those for the full radiation and Kain-Fritsch cumulus parameterizations, passed initial validation tests. The adjoint code will be used to perform adjoint sensitivity studies and the results will be compared to those obtained using very-large-ensemble methods. A 4DVAR data assimilation system can also be built using this adjoint code.

### ***3.15 Retrieval of the soil model initial state using 4DVAR method and improvement of land-surface model***

Ren and Xue (2004), under partial support of this project, proposed an improvement to the temperature prediction equation used in land-surface models based on the force-restore model. It was shown that the improved system produced much better predictions of deep-layer soil temperatures, and the modification was found important for the 4DVAR-based soil temperature and moisture retrieval work (Ren 2004). In another work (Ren et al. 2004) hydraulic lift was introduced into a multi-layer soil-hydrology model that enabled that model to correctly predict daytime moistening and night-time drying in the near-surface soil under dry conditions.

## **4 Education and Training**

Overall, this research grant provided support for six Ph.D. students (H. Liu, M. Tong, and P. Nutter, D. Dawson, M. Hu, and Y. Xiao) and two M.S. students (D. Dawson and G. Stano). The participation of D. Dawson, G. Stano, P. Nutter, leveraged significantly on their fellowships, the National Defense Science and Engineering and NSF Fellowships (Dawson) and the Williams Fellowships (G. Stano, P. Nutter, and Y. Xiao). This project supported Nutter and Xiao when the Williams Fellowships for them prematurely ended, due to sudden economic hardships of the Williams Company, which had provided their initial support. The grant also supported the research of a post-doctoral scientist W. Martin and visiting post-doctoral scientist J. Min. Under the complete or partial support of this grant, four Ph.D. degrees and two MS degrees were completed. This project also provided training opportunities for five graduate students in fall 2003, who utilized the data produced by this project to perform numerical experimentation using the ARPS model as part of their term project in a Computational Fluid Dynamics course taught by the PI. PIs Xue and Carr twice co-taught a newly developed graduate course on data assimilation and Co-PI Brewster presented a lecture on radar data assimilation at the International Summer School on Atmospheric Data Assimilation (ISSOAS), all making use of the latest research results from this project.

Overall, the project provided training for graduate students and post-doctoral scientists in the strategically important areas of numerical modeling, advanced data assimilation methods and understanding of mesoscale processes, and enabled them to gain improved abilities for performing scientific research and publishing scientific findings.

List of project participants of this project:

Ming Xue	Principal Investigator (PI)
Jidong Gao,	Co-PI

Keith Brewster	Co-PI
Alan Shapiro	Co-PI
Fred Carr	Co-PI
Willam Martin	Post-doctoral scientist
Jinzhong Min	Visiting research scientist
Paul Nutter	Ph.D. student, completed in 2003.
Geoffrey Stano	M.S. student, completed in 2003.
Mingjing Tong	Ph.D. student, completed in 2006.
Haixia Liu	Ph.D. student, current.
Ming Hu	Ph.D. student, completed in 2005.
Ying Xiao	Ph.D. student in Computer Sciences, completed 2005.
Dan Dawson	M.S. (completed in 2004) and (current) Ph.D. student.

## 5 Thesis and Dissertation Completed

Nutter, P., 2003: Effects of nesting frequency and lateral boundary perturbations on the dispersion of limited-area ensemble forecasts, Ph.D. Dissertation, University of Oklahoma, 156 pp.

Martin, W. J., 2003: Measurements and modeling of the Great Plains low-level jet. Ph.D. Dissertation, University of Oklahoma.

Stano, G., 2003: A case study of convective initiation on 24 may 2002 during the IHOP field experiment, M.S. Thesis, University of Oklahoma, 106 pp.

Hu, M., 2005: 3DVAR and cloud analysis with WSR-88D level-II data for the prediction of tornadic thunderstorms, Ph. D. Dissertation, School of Meteorology, University of Oklahoma, 217 pp.

Tong, M., 2006: Ensemble Kalman filter assimilation of Doppler radar data for the initialization and prediction of convective storms, Ph.D. Dissertation, School of Meteorology, University of Oklahoma, 243 pp.

## 6 List of publications completed under complete or partial support of this grant.

Bi, L., A. Shapiro, P. Zhang, and Q. Xu, 2002: Quality control problems for VAD winds and NEXRAD level-II winds in the presence of migrating birds. 15th Conf. Num. Wea. Pred./19th Conf. Wea. Analysis and Forecasting., San Antonio, Texas., Amer. Meteor. Soc.

Brewster, K., 2002: Recent advances in the diabatic initialization of a non-hydrostatic numerical model. Preprints, 15th Conf on Numerical Weather Prediction and 21st Conf on Severe Local Storms, San Antonio, TX, Amer. Meteor. Soc., J6.3.

- Brewster, K., A. Shapiro, J. Gao, E. M. Kemp, P. Robinson, and K. Thomas, 2003: Assimilation of radar data for the detection of aviation weather hazards. Preprints, 31 Conf. on Radar Meteorology, Amer. Meteorol. Society, 339-342.
- Brewster, K. A., 2003a: Phase-correcting data assimilation and application to storm-scale numerical weather prediction. Part I: Method description and simulation testing. *Mon. Wea. Rev.*, **131**, 480-492.
- Brewster, K. A., 2003b: Phase-correcting data assimilation and application to storm scale numerical weather prediction. Part II: Application to a Severe Storm Outbreak. *Mon. Wea. Rev.*, **131**, 493-507.
- Chow, F. K., R. L. Street, M. Xue, and J. H. Ferziger, 2005: Explicit filtering and reconstruction turbulence modeling for large-eddy simulation of neutral boundary layer flow. *J. Atmos. Sci.*, **62**, 2058-2077.
- Chow, F. K., A. P. Weigel, R. L. Street, M. W. Rotach, and M. Xue, 2006: High-resolution large-eddy simulations of flow in a steep Alpine valley. Part I: Methodology, verification and sensitivity studies. *J. Appl. Meteor.*, 63-86.
- Dabberdt, W. F., T. W. Schlatter, F. H. Carr, E. W. Joe Friday, D. Jorgensen, S. Koch, M. Pirone, F. M. Ralph, J. Sun, P. Welsh, J. W. Wilson, and X. Zou, 2005: Multifunctional mesoscale observing networks. *Bull. Amer. Meteor. Soc.*, **86**, 961-982.
- Dawson, D. T., II and M. Xue, 2004: Impact of mesoscale data, cloud analysis on the explicit prediction of a MCS during IHOP 2002. Extended Abstract, 20th Conf. Wea. Analy. Forecasting/16th Conf. Num. Wea. Pred., Seattle, WA, Amer. Meteor. Soc.
- Dawson, D. T., II and M. Xue, 2006: Numerical forecasts of the 15-16 June 2002 Southern Plains severe MCS: Impact of mesoscale data and cloud analysis. *Mon. Wea. Rev.*, **134**, 1607-1629.
- Dowell, D. C. and A. Shapiro, 2003: Stability of an iterative dual-Doppler wind synthesis in Cartesian coordinates. *J. Atmos. Ocean. Tech.*, **20**, 1552-1559.
- Gao, J.-D., M. Xue, K. Brewster, and K. K. Droegemeier, 2003: A 3DVAR method for Doppler radar wind assimilation with recursive filter. 31st Conf. Radar Meteor., Seattle, WA, Amer. Meteor. Soc.
- Gao, J.-D., M. Xue, K. Brewster, and K. K. Droegemeier, 2004a: A three-dimensional variational data analysis method with recursive filter for Doppler radars. *J. Atmos. Ocean. Tech.*, **21**, 457-469.
- Gao, J.-D., K. K. Droegemeier, J.-D. Gong, and Q. Xu, 2004b: A method for retrieving mean horizontal wind profiles from single-Doppler radar observations contaminated by aliasing. *Mon. Wea. Rev.*, **132**, 1399-1409.
- Gao, J. and K. K. Droegemeier, 2004: A wind profile retrieval method from azimuthal gradients of radial velocity. *J. Appl. Meteor.*, **42**, 934-940.
- Gao, J. and M. Xue, 2006a: An efficient dual-resolution approach for ensemble data assimilation and tests with the assimilation of Doppler radar data. *Mon. Wea. Rev.*, To be submitted.
- Gao, J. and M. Xue, 2006b: An efficient dual-resolution ensemble data assimilation approach and tests with the assimilation of Doppler radar data. Extended abstract, 10th Symposium on Integrated Observing and Assimilation Systems for the Atmosphere, Oceans and Land Surface (IOAS-AOLS), Atlanta, GA, Amer. Meteor. Soc.,.
- Gao, J., K. Brewster, and M. Xue, 2006a: A comparison of the radar ray path equations and approximations for use in radar data assimilation. *Adv. Atmos. Sci.*, **23**, 190-198.

- Gao, J., K. Brewster, and M. Xue, 2006b: Sensitivity of radio refractivity to moisture and temperature and its influence on radar ray path. *J. Appl. Meteor. Climatol.*, Submitted.
- Gao, J., M. Xue, K. Brewster, F. Carr, and K. K. Droegemeier, 2002: New development of a 3DVAR system for a nonhydrostatic NWP model. Preprint, 15th Conf. Num. Wea. Pred. and 19th Conf. Wea. Anal. Forecasting, San Antonio, TX, Amer. Meteor. Soc., 339-341.
- Gao, J., M. Xue, S. Y. Lee, K. K. Droegemeier, and A. Shapiro, 2004c: A 3DVAR method for single Doppler velocity retrieval and application to a severe thunderstorm case. 3rd International Ocean-Atmosphere Conf., Beijing, China, Chinese-American Oceanic Atmospheric Association, CDROM, A6.3.
- Gao, J., M. Xue, S. Y. Lee, K. K. Droegemeier, and A. Shapiro, 2006c: A three-dimensional variational method for velocity retrievals from single-Doppler radar observations on supercell storms. *Meteo. Atmos. Phys.*, In press.
- Godfrey, E. S., M. Tong, M. Xue, and K. K. Droegemeier, 2005: Assimilation of simulated network radar data of varied storm types using EnSRF for convective storm analysis and forecasts. Extended abstract, 17th Conf. Num. Wea. Pred., Washington DC, Amer. Meteor. Soc., 13A.1.
- Hu, M., 2005: 3DVAR and cloud analysis with WSR-88D level-II data for the prediction of tornadic thunderstorms, Ph. D. Dissertation, School of Meteorology, University of Oklahoma, 217 pp.
- Hu, M. and M. Xue, 2002: Sensitivity of model thunderstorms to modifications to the environmental conditions by a nearby thunderstorm in the prediction of 2000 Fort Worth tornado case. Preprint, 15th Conf. Num. Wea. Pred. and 19th Conf. Wea. Anal. Forecasting, San Antonio, TX, Amer. Meteor. Soc., 19-22.
- Hu, M. and M. Xue, 2006: Impact of configurations of rapid intermittent assimilation of WSR-88D radar data for the 8 May 2003 Oklahoma City tornadic thunderstorm case. *Mon. Wea. Rev.*, Accepted.
- Hu, M., M. Xue, and K. Brewster, 2006a: 3DVAR and cloud analysis with WSR-88D level-II data for the prediction of Fort Worth tornadic thunderstorms. Part I: Cloud analysis and its impact. *Mon. Wea. Rev.*, **134**, 675-698.
- Hu, M., M. Xue, J. Gao, and K. Brewster, 2004: Prediction of Fort Worth tornadic thunderstorms using 3DVAR and cloud analysis with WSR-88D Level-II data. 11th Conf. Aviation, Range, Aerospace and 22nd Conf. Severe Local Storms, Amer. Meteor. Soc., CDROM, J1.2.
- Hu, M., M. Xue, J. Gao, and K. Brewster, 2006b: 3DVAR and cloud analysis with WSR-88D level-II data for the prediction of Fort Worth tornadic thunderstorms. Part II: Impact of radial velocity analysis via 3DVAR. *Mon. Wea. Rev.*, **134**, 699-721.
- Jung, Y., M. Xue, G. Zhang, and J. Straka, 2006: Assimilation of polarimetric radar data using ensemble Kalman filter: Direct assimilation with simulated data. *J. Atmos. Sci.*, To be submitted.
- Liu, H. and M. Xue, 2004: 3DVAR retrieval of 3D moisture field from slant-path water vapor observations of a high-resolution hypothetical GPS network. Extended Abstract, 20th Conf. Wea. Anal. Forecasting/16th Conf. Num. Wea. Pred., Seattle, WA, Amer. Meteor. Soc.
- Liu, H. and M. Xue, 2006a: Retrieval of moisture from slant-path water vapor observations of a hypothetical GPS network using a three-dimensional variational scheme with anisotropic background error. *Mon. Wea. Rev.*, **134**, 933-949.

- Liu, H. and M. Xue, 2006b: Prediction of convective initiation and storm evolution on 12 June 2002 during IHOP. Part I: Control simulation and sensitivity experiments. *Mon. Wea. Rev.*, To be submitted.
- Liu, H., M. Xue, R. J. Purser, and D. F. Parrish, 2006a: Retrieval of moisture from simulated GPS slant-path water vapor observations using 3DVAR with anisotropic recursive filters. *Mon. Wea. Rev.*, Accepted.
- Liu, S., M. Xue, and Q. Xu, 2006b: Using wavelet analysis to detect tornadoes from Doppler radar radial-velocity observations. *J. Atmos. Ocean Tech.*, Accepted.
- Lyons, E. J., V. Lakamraju, K. Brewster, M. Xue, and K. D. Hondl, 2005: An end-to-end emulation of the CASA radar network. 32nd Conf. Radar Meteor., Albuquerque, NM, Amer. Meteor. Soc., CDROM 14R.3.
- Martin, W. J. and M. Xue, 2004: Initial condition sensitivity analysis of a mesoscale forecast using very-large ensembles. Extended Abstract, 20th Conf. Wea. Anal. Forecasting/16th Conf. Num. Wea. Pred., Seattle, WA, Amer. Meteor. Soc.
- Martin, W. J. and A. Shapiro, 2005: Impact of Radar Tilt and Ground Clutter on Wind Measurements in Clear Air. *J. Atmos. Ocean. Tech.*, **22**, 649-663.
- Martin, W. J. and M. Xue, 2006a: Determining sensitivities, impacts and covariances from very large ensembles with randomly perturbed initial conditions. *Mon. Wea. Rev.*, To be submitted.
- Martin, W. J. and M. Xue, 2006b: Evolved and random perturbation methods for calculating model sensitivities and covariances. *Mon. Wea. Rev.*, To be submitted.
- Martin, W. J. and M. Xue, 2006c: Initial condition sensitivity analysis of a mesoscale forecast using very-large ensembles. *Mon. Wea. Rev.*, **134**, 192–207.
- May, R. M., M. I. Biggerstaff, and M. Xue, 2006: A Doppler radar emulator and its application to the study of tornadic signature detectability. *J. Atmos. Ocean. Tech.*, Submitted.
- Nutter, P., 2003: Effects of nesting frequency and lateral boundary perturbations on the dispersion of limited-area ensemble forecasts, Ph.D. Dissertation, School of Meteorology, University of Oklahoma, 156 pp.
- Nutter, P., D. Stensrud, and M. Xue, 2002: Effects of nesting frequency and lateral boundary perturbations on the dispersion of limited-area ensemble forecasts. Preprint, 15th Conf. Num. Wea. Pred. and 19th Conf. Wea. Anal. Forecasting, San Antonio, TX, Amer. Meteor. Soc., 312-315.
- Nutter, P., D. Stensrud, and M. Xue, 2004a: Effects of coarsely-resolved and temporally-interpolated lateral boundary conditions on the dispersion of limited-area ensemble forecasts. *Mon. Wea. Rev.*, **132**, 2358-2377.
- Nutter, P., M. Xue, and D. Stensrud, 2004b: On the need for perturbed LBCs in limited-area ensemble forecasts. Extended Abstract, 20th Conf. Wea. Anal. Forecasting/16th Conf. Num. Wea. Pred., Seattle, WA, Amer. Meteor. Soc.
- Nutter, P., M. Xue, and D. Stensrud, 2004c: Application of lateral boundary condition perturbations to help restore dispersion in limited area ensemble forecasts. *Mon. Wea. Rev.*, **132**, 2378-2390.
- Potvin, C. K., A. Shapiro, T.-y. Yu, and M. Xue, 2006: Using a low-order model to characterize tornadoes in multiple Doppler radar data. Preprint, 22nd Int. Conf. Interactive Info. Proc. Sys. Meteor. Oceanogr. Hydro., Atlanta, Amer. Meteor. Soc., CDROM 11.5.
- Ren, D., 2004: 4DVAR Retrieval of Prognostic Land Surface Model Variables, Ph. D. Dissertation, School of Meteorology, University of Oklahoma, 228 pp.

- Ren, D. and M. Xue, 2004: A revised force-restore model for land-surface modeling. *J. App. Meteor.*, **43**, 1768-1782.
- Ren, D. and M. Xue, 2006: Variational assimilation of ground surface temperature for the estimation of state variables of a land surface model. *J. App. Meteor.*, To be submitted.
- Ren, D., M. Xue, and A. Henderson-Sellers, 2004: The effects of hydraulic lift in simulating superficial soil moisture for vegetated surfaces under dry conditions. *J. Hydrometeorol.*, **5**, 1181-1191.
- Shapiro, A., P. Robinson, and J. Wurman, 2002: Rapid-scan single-Doppler velocity retrieval of a thunderstorm outflow. Preprint, 15th Conf. Num. Wea. Pred./19th Conf. Wea. Analysis Forecasting, San Antonio, Texas, Amer. Meteor. Soc.
- Shapiro, A., P. Robinson, J. Wurman, and J. Gao, 2003: Single-Doppler velocity retrieval with rapid-scan radar data. *J. Atmos. Ocean. Tech.*, **20**, 1758-1775.
- Sharif, H. O., F. L. Ogden, W. F. Krajewski, and M. Xue, 2002: Numerical simulations of radar-rainfall error propagation. *Water Resources Research*, **38**, 1140, doi:10.1029/2001WR000525.
- Sharif, H. O., F. L. Ogden, W. F. Krajewski, and M. Xue, 2004: Statistical analysis of radar-rainfall error propagation. *J. Hydrometeorol.*, **5**, 199-212.
- Sheng, C., S. Gao, and M. Xue, 2006: Short-term prediction of a heavy precipitation event by assimilating Chinese CINRAD radar reflectivity data using complex cloud analysis. *Meteo. Atmos. Phys.*, Accept.
- Souto, M. J., C. F. Balseiro, V. Pérez-Muñuzuri, M. Xue, and K. Brewster, 2003: Importance of cloud analysis and impact for daily forecast in terms of climatology of Galician region, Spain. *J. App. Meteor.*, **42**, 129-140.
- Stano, G., 2003: A case study of convective initiation on 24 may 2002 during the IHOP field experiment, M.S. Thesis, School of Meteorology, University of Oklahoma, 106 pp.
- Tong, M., 2006: Ensemble Kalman filter assimilation of Doppler radar data for the initialization and prediction of convective storms, Ph.D. Dissertation, School of Meteorology, University of Oklahoma, 243 pp.
- Tong, M. and M. Xue, 2004: Ensemble Kalman filter assimilation of Doppler radar data with a compressible nonhydrostatic model. Extended Abstract, 20th Conf. Wea. Analy. Forecasting/16th Conf. Num. Wea. Pred., Seattle, WA, Amer. Meteor. Soc.
- Tong, M. and M. Xue, 2005a: Simultaneous retrieval of microphysical parameters and atmospheric state variables with radar data and ensemble Kalman filter method. Preprint, 17th Conf. Num. Wea. Pred., Washington DC, Amer. Meteor. Soc., CDROM P1.30.
- Tong, M. and M. Xue, 2005b: Ensemble Kalman filter assimilation of Doppler radar data with a compressible nonhydrostatic model: OSS Experiments. *Mon. Wea. Rev.*, **133**, 1789-1807.
- Tong, M. and M. Xue, 2006a: Simultaneous estimation of microphysical parameters and atmospheric state with radar data and ensemble square-root Kalman filter. Part II: Parameter estimation experiments. *J. Atmos. Sci.*, Submitted.
- Tong, M. and M. Xue, 2006b: Simultaneous estimation of microphysical parameters and atmospheric state with radar data and ensemble square-root Kalman filter. Part I: Sensitivity analysis and parameter identifiability *J. Atmos. Sci.*, Submitted.
- Weigel, A. P., F. K. Chow, M. W. Rotach, R. L. Street, and M. Xue, 2006: High-resolution large-eddy simulations of flow in a steep Alpine valley. Part II: Flow structure and heat budget. *J. Appl. Meteor.*, **45**, 87-107.

- Xiao, Y., M. Xue, and J. Gao, 2004: Development of adjoint for a complex atmospheric model, the ARPS, using TAF. Extended abstract, 4th Int. Conf. Automatic Differentiation, Chicago.
- Xiao, Y., M. Xue, W. J. Martin, and J. Gao, 2005: Development of an adjoint for a complex atmospheric model, the ARPS, using TAF. *Automatic Differentiation: Applications, Theory, and Implementations*, H. M. Bücker, G. F. Corliss, P. Hovland, U. Naumann, and B. Norris, Eds., Springer, 263-272.
- Xu, Q., S. Liu, and M. Xue, 2006: Background error covariance functions for vector wind analysis using Doppler radar radial-velocity observations. *Quart. J. Roy. Meteor. Soc.*, Conditionally accepted.
- Xue, M., 2002: Density currents in shear flows: Effects of rigid lid and cold-pool Internal circulation, and application to squall line dynamics. *Quart. J. Roy. Met. Soc.*, **128**, 47-74.
- Xue, M., 2004: Tornadogenesis within a simulated supercell storm. Abstract, 22nd Conf. Severe Local Storms., Hyannis, Massachusetts., Amer. Meteor. Soc.
- Xue, M. and J. Min, 2003: Precipitation verification on CAPS Real-time forecasts during IHOP 2002. Presentation, IHOP Spring Science Meeting, Boulder CO.
- Xue, M. and D. Ren, 2006: Estimation of soil model state through variational assimilation of near surface atmospheric measurements. *J. App. Meteor.*, To be submitted.
- Xue, M. and H. Liu, 2006: Prediction of convective initiation and storm evolution on 12 June 2002 during IHOP. Part II: High-resolution simulation and mechanisms of convective initiation, To be submitted.
- Xue, M. and W. J. Martin, 2006a: A high-resolution modeling study of the 24 May 2002 case during IHOP. Part II: Horizontal convective rolls and convective initiation. *Mon. Wea. Rev.*, **134**, 172–191.
- Xue, M. and W. J. Martin, 2006b: A high-resolution modeling study of the 24 May 2002 case during IHOP. Part I: Numerical simulation and general evolution of the dryline and convection. *Mon. Wea. Rev.*, **134**, 149–171.
- Xue, M., M. Tong, and M. Hu, 2005a: Assimilation of Radar Data for Thunderstorm Prediction with Ensemble Kalman Filter Method. Abstract, 4th WMO Int. Symp. Assimilation Obs. Meteor. Ocean., Prague, Czech Republic.
- Xue, M., M. Tong, and K. K. Droegemeier, 2005b: Impact of radar configuration and scan strategy on assimilation of radar data using ensemble Kalman filter. 9th Symp. Integrated Obs. Assim. Sys. Atmos. Oceans Land Surface, San Diego, California, Amer. Meteor. Soc., CDROM, 9.3.
- Xue, M., M. Tong, and K. K. Droegemeier, 2006a: An OSSE framework based on the ensemble square-root Kalman filter for evaluating impact of data from radar networks on thunderstorm analysis and forecast. *J. Atmos. Ocean Tech.*, **23**, 46–66.
- Xue, M., S. Liu, and T. Yu, 2006b: Variational analysis of over-sampled dual-Doppler radial velocity data and application to the analysis of tornado circulations. *J. Atmos. Ocean Tech.*, Accepted.
- Xue, M., D.-H. Wang, J.-D. Gao, K. Brewster, and K. K. Droegemeier, 2003: The Advanced Regional Prediction System (ARPS), storm-scale numerical weather prediction and data assimilation. *Meteor. Atmos. Physics*, **82**, 139-170.
- Xue, M., K. Brewster, D. Weber, K. W. Thomas, F. Kong, and E. Kemp, 2002: Realtime storm-scale forecast support for IHOP 2002 at CAPS. Preprint, 15th Conf. Num. Wea. Pred. and 19th Conf. Wea. Anal. Forecasting, San Antonio, TX, Amer. Meteor. Soc., 124-126.